AN ANALYTIC INVESTIGATION OF FLOW AND HEMOLYSIS IN PERISTALTIC-TYPE BLOOD PUMPS

by

James R. Meginniss

B.E.S., Johns Hopkins University

(1968)

Submitted in Partial Fulfillment

of the Requirements for the

Degree of

Master of Science

at the

MASSACHUSETTS INSTITUTE OF TECHNOLOGY

June, 1970

Signature redacted

Signature of Author . . . . . .
Department of Mechanical Engineering

Signature redacted

Certified by. . . . . .
Thesis Supervisor

Signature redacted

Accepted by . . . . . .
Chairman, Departmental Committee on Graduate Students

AN ANALYTIC INVESTIGATION OF FLOW AND HEMOLYSIS IN PERISTALTIC-TYPE BLOOD PUMPS

by

James R. Meginniss

Submitted to the Department of Mechanical Engineering
in partial fulfillment of the requirements
for the degree of
Master of Science

ABSTRACT

An analytical model for the flow of blood in roller pumps is developed for the case when inertial forces are small in comparison with viscous forces. The pressure--flow characteristic of the pump and the shear stress distribution on the tube wall are determined as functions of the geometrical and dynamical parameters. A criterion permitting relative comparisons of the rate of hemolysis produced by roller pumps of various designs is derived with the assumption that the wall shear stress is the main agent of hemolysis. According to this criterion, the hemolysis index is minimum when the roller is set so that the minimum gap in the compressed tube is typically of the order of 50 microns.

Thesis Supervisor: Michel Y. Jaffrin

Title: Assistant Professor of Mechanical Engineering

ACKNOWLEDGEMENTS

The author would like to thank Prof. Michel Y. Jaffrin for his patient assistance and valuable suggestions which greatly aided in the development of the theory in this paper. The author would also like to thank Prof. Ascher H. Shapiro, who provided many helpful concepts.

TABLE OF CONTENTS

NOMENCLATURE

a =semi-major axis of elliptical transverse tube cross-section

A $=\frac{a}{R}$

$\overline{AB}$ =time or space average over one full wavelength of A·B; see Eq. (3.25)

b =semi-minor axis of elliptical transverse tube cross-section

B $=\frac{b}{R}$

c =wave speed

C(Z,t) =limits of integration over cross-section of tube at (Z,t)

d =dimensionless effective roller radius = (dimensionless roller radius) + (dimensionless tube wall thickness)

D $=(\frac{A^2-B^2}{A^2})$; see Appendix 2

E =complete elliptic integral of Second Kind; see Eq. (A 2.1)

F =dimensionless flow in wave frame $=\left(\frac{q}{\pi R^2 c}\right)$

F° =Witch of Agnesi pumping parameter; see Eq. (3.26)

G(u) =function defined by Eq. (A 5.8)

G° =Witch of Agnesi pumping parameter; see Eq. (3.27)

h =dimensionless major axis of transverse cross-section of undeformed tube = $2 \cdot B_{maximum}$

H =function of (X,Y,Z,t); H=0 gives shape of inside surface of tube

Hb =hemoglobin

I.H. =index of hemolysis

$J(x,y) = \left[\frac{x^2}{a^2} + \frac{(y-b)^2}{b^2} - 1\right]$; see Eq. (A 3.3)

k = (subscript) denotes a quantity evaluated in the compressed region (i.e., in the "well") of a square wave

k* ="surface interaction coefficient" for hemolysis criterion; see Eq. (4.9)

K(B,A) =adjustment factor for average shear stress; see Eqs. (4.21) and (4.22)

$L = \frac{\lambda}{R}$

m =shape parameter in modified Witch of Agnesi wave (usually, m=0.4); see Eq.(3.39)

n =inner normal coordinate direction from wall; see Eq. (4.10)

$\underline{n} = (n_x, n_y)_{wall}$ = unit inner normal vector to wall (in x-y cross-section); see Eq. (A 3.1)

O =order of magnitude of, e.g., $O(\epsilon^3)$ = order of magnitude of ϵ^3

p =pressure measured in wave frame

P =perimeter of elliptical cross-section = $2\pi R$

q =volume rate of flow in wave frame

Q =volume rate of flow in lab frame

$\bar{Q}$ = space average over one wave length, or time average over one wave period, of volume rate of flow in lab frame

$\bar{Q}_{max}$ =maximum $\bar{Q}$ compatible with Re** = 1; see Eqs. (5.54)-(5.58)

r = (1) radial coordinate in straight circular cylindrical tube;
(2) quantity defined by Eq. (4.43)

R =internal radius of undeformed tube = radius of circle having perimeter equal to perimeter of elliptical cross-section (all lengths are non-dimensionalized by dividing by R)

Re =approximate Reynolds Number = ratio of inertia to viscous terms of Navier Stokes Equation; see Eq. (5.18)

Re** =maximum Reynolds Number on centerline of tube; see Eq. (5.48)

R_T =radius of straight circular cylindrical tube

S = (1) dimensionless length of compressed region of square wave;
(2) arc length

t =time

u =horizontal transverse fluid velocity measured in wave frame

U =horizontal transverse fluid velocity measured in lab frame

V =vertical fluid velocity measured in lab frame

v =vertical fluid velocity measured in wave frame

w =longitudinal fluid velocity measured in wave frame

w_o =waveframe longitudinal centerline velocity; see Eq.(5.6)

W =longitudinal fluid velocity measured in lab frame

x =wave frame transverse (horizontal) coordinate

X =lab frame transverse (horizontal) coordinate

$X(z)$ =limits of integration over cross-section of tube at z in wave frame

$X(z,t)$ =limits of integration over cross-section of tube at z in wave frame at time t

y =wave frame transverse (vertical) coordinate

y_{max} $=Y_{max}(Z-ct)$ = dimensional wave shape in wave frame; see Eq. (2.11)

Y =lab frame transverse (vertical) coordinate

$Y_{max}(Z,t)$=dimensional wave shape in lab frame; see Eq. (2.10)

η $=\frac{z}{R}$

η_o = an intermediate limit of integration in evaluating I.H. for modified Witch of Agnesi Wave Shape; see Eq. (A 4.1)

η^* =value of η at"truncation point" in Witch of Agnesi Wave Shape

η^{**} =value of η when Re=Re**, (apart from region of Reynolds Number singularity); see Eq. (5.47)

z =$Z-ct$ = waveframe longitudinal coordinate

Z =lab frame longitudinal coordinate

α = (1) a specific constant which probably lies between 0.7 and 1.7 :

$A = A(B) \cong \frac{\pi}{2} - \alpha \cdot B^2$; see Eq. (2.9) and Appendix 2;

(2) shape parameter in general Witch of Agnesi wave shape; see Eq. (2.14);

(3) coefficient in Eq. (5.48)

β =shape parameter in general Witch of Agnesi wave shape

γ =shape parameter in general Witch of Agnesi wave shape

$\Gamma(Z,t)$ =area of tube cross-section at (Z,t)

δ =shape parameter in general Witch of Agnesi wave shape

δp_1 =pressure rise per wave length

Δx =characteristic horizontal transverse length scale for changes in longitudinal velocity in compressed region of tube; see Eq. (5.8)

Δy =characteristic vertical length scale for velocity changes in compressed region of tube; see Eq. (5.9)

η $=\frac{Y}{R}$

η_{max} $=2 \cdot B$

ϵ =dimensionless minimum gap width = $2 \cdot B_{minimum}$

ϵ_o =value of ϵ that minimizes I.H.

λ = (1) wave length = distance between two rollers;
(2) length of straight, circular cylindrical tube

μ =viscosity of liquid

ν =kinematic viscosity

τ = (1) shear stress in fluid;
(2) characteristic time of flow motion;see Eq. (5.3)

ρ =mass density of liquid

τ_{wall} =shear stress at wall of tube due to longitudinal velocity profile

$(\tau_{wall})_{aver}$ =mean longitudinal shear stress around perimeter of a transverse tube cross-section; see Eq. (4.15)

ξ $=\frac{x}{R}$

ω $=\frac{w}{c}$

∇^2 =dimensionless Laplacian operator; see Eq. (3.1)

1. INTRODUCTION

Peristaltic pumps are used for pumping blood, sterile fluids, corrosive liquids or gases, slurries, and suspensions whenever it is necessary to isolate the transported fluid from the pumping mechanism. This type of pump consists of a flexible tube compressed along a part of its length by a moving roller, a nutating plate or a series of mechanical fingers. Usually, the compressing mechanism occludes the tube completely or almost completely and the pump works by "milking" the fluid through the tube, but complete occlusion is not at all necessary for a peristaltic pump to work; viscous forces can produce effective pumping even if the tube is not occluded, but the volume flow rate then depends upon the pressure head.

This paper is mainly concerned with roller pumps used for pumping blood in extracorporeal circulation during open-heart surgery. A severe disadvantage of these pumps is their high rate of hemolysis (destruction of red blood cells) which, with the hemolysis due to other mechanical components of the extracorporeal blood circuit, limits the duration of pumping to a few hours. There is evidence[1] that the rate of homolysis associated with blood flow through a tube is directly related to the shear rate in the flow.

1.1 Description of Commercially Available Pumps

The 1969-70 Guide to Scientific Instruments[2] of

Science magazine lists 27 manufacturers of peristaltic pumps. Some of these pumps are for general industrial use; others are strictly for medical applications. A survey of the manufacturers' literature reveals a considerable variety of designs, mechanisms, special features, and operating parameters.

Production models of roller pumps have between one[3] and six rollers[4] and maximum flow rates ranging from 0.1 liter/min[4] to 10.0 liters/min[5]; tube diameters range from 3/16 to 5/8 inch (inside).[4,5] Special features available on some roller pumps are: micrometer adjustment devices[3,5] for changing the degree to which the rollers occlude the tube; a resilient back-up plate[4] against which the tubing is compressed during passage of the roller (such a back-up plate reduces tubing wear); an automatic pulsator accessory[3] which periodically interrupts the roller motion to produce a pulsatile flow of any desired rectangular wave shape.

The largest of the commercially available finger pumps[6] accomodates tubing with inside diameter up to 1 inch, and pumps a maximum of 17 liters/min; the design permits pumping through as many as four tubes simultaneously; the tube is completely occluded by the mechanical fingers.

The kinetic clamp pump compresses the tubing between two circular plates, one of which nutates - i.e., wobbles without rotating - to produce on the tube an advancing point of maximum compression. The largest of the kinetic clamp pumps[6] accepts a single tube with inside diameter of up to 1/4 inch, and pumps as much as 1.5 liters/min; occlu-

sion is complete.

Laboratory models of roller pumps with other special design features have been tested; pumps with gear-driven (as opposed to free-rolling) rollers[7], with spring-loaded rollers[8] (as opposed to rollers with degree of occlusion held rigidly constant), with a free-centered roller[7] (as opposed to a roller which rotates about a fixed axis), and with flat, naturally-elliptical and internally-valved tubing.[9]

Most peristaltic pumps are operated in or near the fully-occlusive mode in order to prevent variations of flow rate with changes in pressure rise across the pump and to make the flow rate be directly proportional to the pump cycle speed. In the fully occlusive mode, volume flow rate is approximately given by the transverse cross-sectional area of the undeformed tube multiplied by the velocity of the roller (or other compression mechanism). In the non-fully occlusive mode, which is the more general case (and which is the case treated in this paper), the flow is less than in the fully occlusive mode due to backwards "leakage" flow beneath the point of maximum occlusion. A surgeon describes this circumstance as follows: "Under the pressures encountered in pumping blood through a cannula into the arterial tree (up to 400 mm Hg) calibration of the pump output can be based upon the rate of rotation. Unless the rollers or fingers are set to produce occlusion, it has been shown that the output drops and the pump rate is not a re-

liable index of the actual output as pressure rises".[8]

1.2 Blood Damage Caused by Pumping

"Blood damage" covers a highly complex set of phenomena which include rupture (hemolysis) of some red cells with release of hemoglobin into the plasma, weakening (i.e., sublethal damage) of other red cells, acute decrease in platelet count, and acute increase in the white cell count.[10]

A convenient index (but not an absolute measure) of blood damage is the Index of Hemolysis (I.H.) which is defined as the number of mg of hemoglobin (Hb) released into the plasma per 100 ml of blood pumped. In the normal, average, healthy adult human, the I.H. for the heart and circulatory system is about 0.0868 mg Hb per 100 ml blood pumped by the heart (see Appendix 1 for the calculations leading to this value). The I.H. of blood-handling apparatus and pumps can be compared with this "normal" value of I.H. to determine the relative importance of the blood damage due to the apparatus and pumps.

The factors that cause blood damage in peristaltic pumps (or any other kind of blood-handling apparatus) are only qualitatively described in much of the medical literature. For example, in Ref. 8 it is stated that "...the scrubbing action of one side of the tube against the other and the intense eddy formation which may occur if occlusion is not complete result in hemolysis". In other papers[7,11,12] there are reported empirical measurements of I.H. for particular combinations of geometry, flow, pressure, tubing, etc. But in

all cases a general quantitative, algebraic expression for the relation between geometry, flow pressure, etc., and I.H. is lacking. This paper will develop such an expression for I.H. The general purpose of the present investigation is to analytically predict the pumping performance and hemolysis characteristics of roller-type peristaltic blood pumps as a function of the relevant geometric and dynamic parameters.

2. GEOMETRY

2.1 General Considerations

As unambiguous definition of the geometry of the peristaltic pump is a necessary precondition for the analytic determination of the pump's dynamic characteristics (e.g., velocity profile, pressure vs. flow relation, shear stress distribution, hemolysis index criterion, etc.). A sufficient geometrical specification would be a function giving at all times the complete three-dimensional shape of the inside surface of the tube (which contains the liquid). Such a function could be represented as

$$H(X,Y,Z,t) = 0 \tag{2.1}$$

where X, Y, Z are rectangular coordinates in the lab frame, and t is time. To obtain H for an actual tube would require an analysis of the problem of large deformation of an elastic tube with finite wall thickness. Such considerations would be too complex for a study such as this, so a simplified approach, yielding an approximate expression for H, has been devised. The simplified geometric approach rests upon three assumptions: that the centerline of the undeformed tube is straight, that all the transverse cross-sections of the inner surface of the tube are ellipses, and that these ellipses are of constant and equal perimeter (but of varying eccentricities). The centerline of the undeformed tube is assumed to be straight because the internal radius of the

tube is small in comparison with the radius of the pump. Thus secondary flows due to centerline curvature are neglected. The ellipse is chosen as the approximation to the cross-sectional shape because, except for the circle, the ellipse is analytically the simplest of the two-dimensional closed curves and the Poiseuille velocity distribution in a tube of elliptical cross-section is known. Each transverse (elliptical) cross-section is characterized by a semi-major axis "a" and a semi-minor axis "b". The constant-perimeter assumption yields a functional relationship between "a" and "b". At this point, to complete the specification of H(X,Y,Z,t) it is only necessary to specify

$$b = b(Z,t) \tag{2.2}$$

the longitudinal and time variation of the semi-minor axis (which is the axis being compressed in the pump).

2.2 Shape of the Compressed Tube

A. Elliptical Cross-Sections

Assuming that the lowest point of each cross-section lies on the Z - axis, the equation of the elliptical cross-sections is

$$\frac{X^2}{a^2} + \frac{(Y-b)^2}{b^2} = 1 \tag{2.3}$$

B. Constant-Perimeter Condition

The perimeter, P, of the ellipse represented by Eq. (2.3) is given by the Complete Elliptic Integral of the Second Kind:

$$P = 4a\int_0^{\pi/2}\left[1 + \left(\frac{b^2-a^2}{a^2}\right)\sin^2 w\right]^{1/2} dw \qquad (2.4)$$

which can be expanded as an infinite series[13]:

$$P = \pi(a+b)\left[1 + \frac{1}{2^2}\left(\frac{a-b}{a+b}\right)^2 + \frac{1^2}{2^2 4^2}\left(\frac{a-b}{a+b}\right)^4 + \frac{1^2 3^2}{2^2 4^2 6^2}\left(\frac{a-b}{a+b}\right)^6 + \cdots\right] \qquad (2.5)$$

If R is the radius of the circle which has the same perimeter as the ellipse of Eq. (2.3), and defining dimensionless variables:

$$A \equiv \frac{a}{R} \quad , \quad B \equiv \frac{b}{R} \qquad (2.6)$$

then the constant-perimeter condition, using Eq. (2.5), yields

$$2 = (A+B)\left[1 + \frac{1}{4}\left(\frac{A-B}{A+B}\right)^2 + \frac{1}{64}\left(\frac{A-B}{A+B}\right)^4 + \cdots\right] \qquad (2.7)$$

On keeping only the first two terms of Eq. (2.7) (since the series converges very rapidly), and solving for A in terms of B, the following expression is obtained:

$$A \cong \frac{1}{5}\left[-3\cdot B + 4 + 4\cdot\left(1-B^2+B\right)^{1/2}\right] \qquad (2.8)$$

for $A \geq B$.

The approximate value of A given by Eq. (2.8) differs from the exact value by 1.86% at most. The error is maximum at B = 0. For $B << 1$, a more accurate expression is:

$$A \cong \left(\frac{\pi}{2} - \alpha\cdot B^2\right) \quad , \quad B << 1 \qquad (2.9)$$

where α is a constant between 0.7 and 1.7 (see Appendix 2).

Figure 1 shows a comparison of the "exact" constant-perimeter relation A = A(B) given implicitly by Eq. (2.4) and of the approximate one given by Eq. (2.8).

Figure 2 shows a family of constant-perimeter ellipses, of the form of Eq. (2.3).

C. Wave Shape

The shape of the longitudinal vertical mid-section of the tube is called the "wave-shape" and is specified by

$$Y = Y_{max}(Z,t) = 2 \cdot b(Z,t) \qquad (2.10)$$

(Eq. (2.10) is obtained by substituting Eq. (2.2) into (2.3) and setting X = 0.)

For an idealized roller pump, Y_{max} is a wave of unchanging shape propagating along the tube at a constant velocity, c. Y_{max} is produced by the roller(s) compressing the tube.

Real roller pumps are so designed that there is always at least one roller compressing the tube. Each roller periodically comes into contact with the tube, compresses the tube while rolling along a certain length of the tube, and then separates from the tube. Except when the roller first meets the tube or when it leaves it, the wave shape produced by the moving roller(s) is (very nearly) constant. Therefore, if (as in most actual roller pumps) the time duration of the contacting and separating stages is short compared to the time duration of the steady rolling-compression stage, then, as a reasonably good first approximation, the wave shape may be assumed to be constant for all t. This assumption, combined with a coordinate transformation:

$$\begin{aligned} x &\equiv X \\ y &\equiv Y, \quad y_{max} \equiv Y_{max} \\ z &\equiv (Z - ct) \end{aligned} \tag{2.11}$$

and with a definition of dimensionless coordinates

$$\begin{aligned} \xi &\equiv x/R \\ \eta &\equiv y/R, \quad \eta_{max} \equiv y_{max}/R \\ \zeta &\equiv z/R \end{aligned} \tag{2.12}$$

and with Eq. (2.6), converts Eq. (2.10) into the form

$$\eta = \eta_{max} = 2 \cdot B(\zeta) \tag{2.13}$$

The frame (x,y,z) defined by Eq. (2.11) is called the "wave frame". In the wave frame, the wave shape, given in dimensionless form by Eq. (2.13), is steady (i.e., fixed in shape

and position).

Figure 3 illustrates a wave shape qualitatively typical of roller pumps. In Figure 3, the wave shape is regarded as being symmetric about $\eta = 0$. "ϵ" is the dimensionless gap width at the point of maximum compression.* "d" is the dimensionless effective roller radius (approximately equal to the actual dimensionless roller radius plus the dimensionless thickness of the tube wall) -- equal to the dimensionless radius of curvature of the wave at $\eta = 0$. "h" is the dimensionless diameter of the undeformed tube; for a naturally circular tube, h = 2.0; for a naturally elliptical tube, h $\neq$ 2.0.

Two basic wave shapes will be considered in this paper: the "Witch of Agnesi" shape and the "Square" shape. The Witch of Agnesi wave shape (so called because of its resemblance to the classical curve of the same name) is a close approximation to the wave shape of conventional roller pumps. The Square wave shape, which cannot be produced by a circular roller, permits simpler calculations and is an interesting case for comparative purposes.

The Witch of Agnesi wave has an equation of the general form

$$\eta = \eta_{max}(\eta) = \left[\frac{\alpha \cdot \eta^2 + \beta}{\gamma \cdot \eta^2 + \delta}\right] \qquad (2.14)$$

Only three of the four coefficients, α, β, γ, δ, are independent, so only three geometric conditions need be speci-

* All lengths are non-dimensionalized by dividing by R.

fied in order to determine them. These geometric conditions are (see Figure 4):

$$\epsilon = \eta_{max}(0) \tag{2.15}$$

$$d = \text{radius of curvature of } \eta_{max}(\zeta) \text{ at } \zeta = 0 \tag{2.16}$$

$$h = \eta_{max}(\zeta^*) \tag{2.17}$$

The best fit of Eq. (2.14) to a conventional roller pump wave shape is obtained by truncating the Witch of Agnesi at a finite ζ^*, and assuming that the tube is cylindrical for $|\zeta| \geq \zeta^*$, so that

$$\eta = \eta_{max}(\zeta) = h \quad , \qquad \text{when} \qquad |\zeta| \geq \zeta^* \tag{2.18}$$

The value of ζ^* depends upon the elastic properties of the tube and must be determined empirically. (A typical value is $\zeta^* = 8$.)

Solving for α, β, γ, and δ in terms of ϵ, d, h, and ζ^*, and combining Eq. (2.14) with (2.18), the following expression is obtained for the Witch of Agnesi wave shape:

$$\eta = \eta_{max}(\zeta) = 2 \cdot B(\zeta) = \begin{cases} \dfrac{\left[\left[h\zeta^{*2} - 2(h-\epsilon)d\epsilon\right]\zeta^2 + \left[2(h-\epsilon)d\epsilon\zeta^{*2}\right]\right]}{\left[\left[\zeta^{*2} - 2(h-\epsilon)d\right]\zeta^2 + \left[2(h-\epsilon)d\zeta^{*2}\right]\right]}, \\ \qquad \text{for} \quad \zeta^2 \leq \zeta^{*2} \ ; \\ h, \quad \text{for} \quad \zeta^2 \geq \zeta^{*2} \end{cases} \tag{2.19}$$

Note that the derivative, $\frac{d\eta_{max}}{d\zeta}$, is discontinuous at $\zeta = \zeta^*$. This discontinuity in slope is of negligible importance.

Since ϵ, d, h, and ζ^* are independent parameters, Eq. (2.19) is effectively a four-parameter fit to the conventional roller pump wave shape.

The osculating parabola to Eq. (2.19) is obtained by taking the limit of Eq. (2.19) as $h \to \infty$ (necessitating, by Eq. (2.17), that $\zeta^* \to \infty$ also). The osculating parabola thus obtained is:

$$\eta = \eta_{max}(\zeta) = \left[\frac{1}{2 \cdot d} \cdot \zeta^2 + \epsilon\right] \qquad (2.20)$$

which is a very good approximation to the Witch of Agnesi wave shape, Eq. (2.19), when ζ^2 is sufficiently smaller than ζ^{*2}, or (equivalently), when η_{max} - as computed by Eq. (2.19) - is sufficiently smaller than h. Eq. (2.20) will turn out to be very useful in Sections 3.3D, 4.4, and 5. Figure 5 shows a comparison of Eqs. (2.19) and (2.20) for a particular set of dimensionless geometric parameters.

2.3 Empirical Verification of the Geometric Model

A. Constant-Perimeter and Elliptical Cross-Section Assumptions

Several straight, circular cross-section, polyvinyl chloride tubes were filled with wet plaster and compressed transversely at one point with a circular cylinder. After the plaster had hardened, the tube was cut off of each plaster casting, and the casting was sliced transversely to

display its cross-sections. Outlines of representative plaster cross-sections are shown in Figures 6 and 7. These diagrams confirm the assumptions (see Section 2.2) of approximately elliptical shape and constant perimeter, for the degrees of compression shown. For degrees of compression greater than those shown in Figures 6 and 7, the cross-sectional shape may begin to depart from an approximately elliptical shape and become narrower at the middle ($\xi = 0$) than at the ends (near $\xi = A$)[12]. This tendency is barely visible in the narrowest of the cross-sections ($z \cong 1/2$ inch) of Figure 6. No attempt will be made in this paper to correct for this "pinching" effect; the effect can be minimized (or perhaps eliminated) by using special tubing which has thinner walls at the ends (near $\xi = A$) of the cross-sections than at the middle ($\xi = 0$)[9].

B. Photo Studies of Tubes Transversely Compressed by Circular Cylinders

Straight, transparent, polyvinyl chloride tubes with circular cross-sections and uniform wall thicknesses were transversely compressed by horizontal circular cylinders of various diameters. The longitudinal vertical profiles were photographed. From each photo the dimensionless geometry of the longitudinal cross-section of the inner wall in the $\xi = 0$ plane was determined and graphed. For comparison with Eq. (2.19), a value of η^* was estimated from each empirical graph, a value of ϵ was measured, a value of d was calculated (by adding the dimensionless tube wall

thickness to the dimensionless radius of the compressing cylinder), and h was set equal to 2.0 (h = 2.0 for a tube which is naturally round). The corresponding graph of Eq. (2.19) was plotted on the same graph as the dimensionless empirical profile.

This comparison, carried out for three different dimensionless geometric configurations, is displayed in Figures 8, 9, and 10. The results indicate that the shape of the empirical "conventional roller pump" wave shape can be fairly well represented by Eq. (2.19), if a proper choice of η^* is made.

Observe that there is only a *small* discontinuity in slope at η^* on the curves, given by Eq. (2.19), in Figures 8, 9, and 10.

3. PUMPING CHARACTERISTICS

3.1 General Considerations

The basic objective of Section 3 is to find the relationship between pressure rise and flow rate for a peristaltic pump. To do this it is first necessary to find the fluid velocity profile $w(\xi,\eta)$ at each transverse cross-section of the tube in the wave frame. This is done by solving the appropriately simplified Navier-Stokes equations subject to appropriate boundary conditions. [w can be assumed to be independent of time if there is assumed to be an integral number of identical waves between two pressure reservoirs, or if there is assumed to be an infinite train of identical waves on the tube]. Integrating the velocity, w, over each cross-section then gives the volume flow rate, q, through that cross-section, as a function of the local pressure gradient. Continuity requires that at any given time q be identical for all wave frame cross-sections if the wave shape is constant. Transforming to the lab frame, the wave frame *constant* flow, q, is transformed to the lab frame *variable* flow, Q. Averaging Q over one wave length (or over one wave period) yields the average lab frame volume flow rate, $\bar{Q}$. Integrating the pressure gradient over one wave length gives the pressure rise per wave length, δp_λ. The relation thus obtained between $\bar{Q}$ and δp_λ is the desired result.

3.2 Velocity Distribution at Each Cross-Section

The assumption of an integral number of identical waves between two constant-pressure reservoirs, permits analysis of the flow as a steady flow in the wave frame. The assumption is a fairly good approximation to actual roller pumps, except during those phases of the pumping cycle when there may momentarily be a non-integral number of waves on the tube because a roller is coming into contact with or separating from the tube.

Assuming that blood is Newtonian and that $\frac{d(y_{max})}{dz}$ is always sufficiently small that transverse pressure gradients, transverse velocities, and z-gradients of longitudinal velocity are very small everywhere, then the longitudinal Navier-Stokes equation may be approximately simplified (by elimination of inertia terms and the third viscous term) to the form:

$$0 = \frac{-1}{\rho}\frac{dp}{dz} + \frac{\mu}{\rho}\nabla^2 w \qquad (3.1)$$

where

$$\nabla^2 = \left(\frac{\partial^2}{\partial x^2} + \frac{\partial^2}{\partial y^2}\right)$$

w = longitudinal fluid velocity in wave frame

ρ = fluid density

p = pressure

μ = viscosity of the fluid

The boundary conditions for Eq. (3.1) are:

$$w = -c \text{ , when } \left[\frac{x^2}{a^2} + \frac{(y-b)^2}{b^2}\right] = 1 \tag{3.2}$$

In terms of the dimensionless wave frame coordinates defined by Eq. (2.12), Eqs. (3.1) and (3.2) become

$$0 = -\frac{dp}{d\zeta} + \frac{\mu c}{R}\left(\frac{\partial^2 \omega}{\partial \xi^2} + \frac{\partial^2 \omega}{\partial \eta^2}\right) \tag{3.3}$$

with boundary conditions:

$$\omega = -1 \text{ , when } \left[\frac{\xi^2}{A^2} + \frac{(\eta - B)^2}{B^2}\right] = 1 \tag{3.4}$$

where Eq. (2.6) has been used, and where

$$\omega \equiv \frac{w}{c} = \text{dimensionless longitudinal fluid velocity in wave frame} \tag{3.5}$$

The solution of Eq. (3.3) satisfying (3.4) is:

$$\omega = \left\{-1 - \frac{R}{2\mu c}\cdot\left[\frac{A^2B^2}{A^2+B^2}\right]\cdot\frac{dp}{d\zeta}\cdot\left[1 - \frac{\xi^2}{A^2} - \frac{(\eta-B)^2}{B^2}\right]\right\} \tag{3.6}$$

3.3 Pressure Rise Across Pump vs. Volume Rate of Flow

A. Arbitrary Wave Shape

If, for a particular fluid element, w is the longitudinal velocity measured in the wave frame and W is the longitudinal velocity measured in the lab frame, then, since the wave and lab frames are related by Eq. (2.11), the

relation between w and W is:

$$w(z,t) = w(Z-ct,t) = W(Z,t) - c \tag{3.7}$$

The volume flow rate in the lab frame is defined by:

$$Q(Z,t) \equiv \iint_{C(Z,t)} W(Z,t)\, dX\, dY \tag{3.8}$$

where C(Z,t) designates the limits of integration over the transverse cross-section of the tube at (Z,t).

Using Eq. (3.7), Eq. (3.8) becomes

$$Q(Z,t) = \iint_{C(Z,t)} w(Z-ct,t)\, dX\, dY + c \cdot \iint_{C(Z,t)} dX\, dY \tag{3.9}$$

The volume flow rate in the wave frame is defined as

$$q(z,t) \equiv \iint_{X(z,t)} w(z,t)\, dx\, dy \tag{3.10}$$

where $X(z,t) \equiv C(z + ct, t)$ designates the limits of integration over the tube cross-section at (z,t).

Also,

$$\iint_{C(Z,t)} dX\, dY \equiv \Gamma(Z,t) \tag{3.11}$$

= the area of the tube cross section at (Z, t).

So, on using Eqs. (2.11), (3.10), and (3.11), Eq. (3.9) becomes:

$$Q(Z,t) = q(z,t) + c \cdot \Gamma(Z,t) \tag{3.12}$$

The validity of Eq. (3.12) does *not* depend upon the assumptions of constant wave shape, steady flow in the wave frame, elliptical cross-sections of constant perimeter, or incompressible fluid. (Note: for a wave of changing shape, the wave frame is still defined by Eq. (2.11).)

Now, using the assumptions of constant wave shape, steady flow in the wave frame, and incompressible fluid, the expression for q(z,t) simplifies to:

$$q(z,t) = q = \text{constant} \tag{3.13}$$

And, using the assumptions of constant wave shape and elliptical cross-sections of constant perimeter, and using Eq. (2.11), the following result is obtained:

$$\Gamma(Z,t) = c \cdot \pi \cdot (ab)\Big|_{(Z-ct)} \tag{3.14}$$

So, substituting Eqs. (3.13) and (3.14) into Eq. (3.12), and noting that Z and t enter on the right hand side only together as (Z - ct), Eq. (3.12) becomes:

$$Q(Z-ct) = q + c \cdot \pi \cdot (ab)\Big|_{(Z-ct)} \tag{3.15}$$

The assumptions which led to Eq. (3.13) are also sufficient to reduce Eq. (3.10) to the form:

$$q = \iint_{X(z)} w(z)\,dx\,dy \tag{3.16}$$

where, now, $X(z)$ designates the limits of integration over the (elliptical) cross-section at z in the wave frame.

Substituting Eqs. (3.5) and (3.6) into Eq. (3.16), using Eqs. (2.6) and (2.12), and integrating the result yields the expression:

$$q = \pi\cdot(AB)\Big|_{\zeta}\cdot R^2 c\cdot\left[-1-\frac{R}{4\mu c}\left(\frac{A^2B^2}{A^2+B^2}\right)\frac{dp}{d\zeta}\right]\Bigg|_{\zeta} \tag{3.17}$$

Substituting Eq. (3.17) into (3.15), and solving for dp/dz gives:

$$\frac{dp}{d\zeta} = \frac{-4\mu}{\pi R^3}\cdot\left(\frac{A^2+B^2}{A^3B^3}\right)\Bigg|_{\zeta}\cdot Q(Z-ct) \tag{3.18}$$

where, by Eqs. (2.11) and (2.12),

$$\zeta \equiv \frac{z}{R} = \left(\frac{Z-ct}{R}\right) \tag{3.19}$$

Define:

$\lambda \equiv$ wave length (= distance between rollers on the tube)

$L \equiv \frac{\lambda}{R} =$ dimensionless wave length (3.20)

$\delta p_\lambda \equiv$ pressure rise per wave length in the wave frame

Integrating Eq. (3.18) over a full wavelength in the wave frame gives:

$$\delta p_\lambda = \int_{-L/2}^{+L/2} \frac{dp}{d\eta}\, d\eta = \frac{-4\mu}{\pi R^3} \cdot \int_{-L/2}^{+L/2} \left(\frac{A^2+B^2}{A^3 B^3} \right)\Bigg|_\eta \cdot Q(Z-ct)\, d\eta \tag{3.21}$$

But, using Eqs. (3.19) and (2.6), Eq. (3.15) becomes:

$$Q(Z-ct) = q + c \cdot \pi \cdot R^2 \cdot (AB)\Big|_\eta \tag{3.22}$$

Substituting Eq. (3.22) into (3.21) yields:

$$\delta p_\lambda = \frac{-4\mu}{\pi R^3} \cdot \left\{ q \cdot \int_{-L/2}^{+L/2} \left(\frac{A^2+B^2}{A^3 B^3} \right)\Bigg|_\eta d\eta + c \cdot \pi \cdot R^2 \cdot \int_{-L/2}^{+L/2} \left(\frac{A^2+B^2}{A^2 B^2} \right)\Bigg|_\eta \cdot d\eta \right\} \tag{3.23}$$

Pressures, and pressure gradients, are invariant under a Galilean velocity transformation, so δp_λ, the pressure rise per wavelength in the wave frame, is also equal to the pressure rise per wavelength in the lab-frame. Therefore Eq. (3.23) holds for either the wave or lab frame.

If Eq. (3.22) is spatially averaged over one wavelength (or if the time average is taken over one wave period), then the result is:

$$\bar{Q} = q + c \cdot \pi \cdot R^2 \overline{AB} \tag{3.24}$$

where the bar($\bar{\ }$) denotes an averaged quantity. q is constant, so its average value is equal to q. $\overline{AB}$ is defined as:

$$\overline{AB} \equiv \frac{1}{L} \cdot \int_{-L/2}^{+L/2} (AB)\Big|_z \cdot dz \tag{3.25}$$

$\bar{Q}$ is analogously defined.

Now define the quantities:

$$F^\circ \equiv \int_{-L/2}^{+L/2} \left(\frac{A^2+B^2}{A^3 B^3}\right)\Big|_z \cdot dz \tag{3.26}$$

$$G^\circ \equiv \int_{-L/2}^{+L/2} \left(\frac{A^2+B^2}{A^2 B^2}\right)\Big|_z \cdot dz \tag{3.27}$$

Then, solving Eq. (3.23) for q, substituting the resulting expression for q into Eq. (3.24), using Eqs. (3.26) and (3.27), and dividing through by $\pi R^2 c$, gives:

$$\left(\frac{\bar{Q}}{\pi R^2 c}\right) = \left[\frac{-\delta P_1}{\mu c/R} \cdot \frac{1}{4F^\circ} + \overline{AB} - \frac{G^\circ}{F^\circ}\right] \tag{3.28}$$

Eq. (3.28) gives the relation between the (time or spatial) mean volume rate of flow in the lab frame and the pressure rise per wave length due to the motion of an infinite train of waves (or an integral number of waves between two pressure reservoirs) of arbitrary but constant shape on a straight tube with elliptical transverse cross-sections of constant perimeter.

B. Witch of Agnesi Wave Shape

The coefficients, $(\frac{1}{4F^\circ})$ and $(\overline{AB} - \frac{G^\circ}{F^\circ})$, in Eq. (3.28) can be computed for the Witch of Agnesi wave shape by substituting Eqs. (2.19) and (2.8) into Eqs. (3.25), (3.26) and (3.27), and then integrating numerically for specific values of L, h, ϵ, d, and ζ^*.

See Table 2 for a tabulation of computed values.

C. Square Wave Shape

The square wave shape, defined as:

$$\eta = \eta_{max}(\zeta) = 2 \cdot B(\zeta) = \begin{cases} \epsilon, & \text{for } 0 \leq |\zeta| < S/2 \\ h, & \text{for } S/2 < |\zeta| \leq L/2 \end{cases} \tag{3.29}$$

permits an analytic calculation of the coefficients $(\frac{1}{4F^\circ})$ and $(\overline{AB} - \frac{G^\circ}{F^\circ})$. Eq. (3.29) is diagramed in Figure 11.

The square wave shape may be thought of as an oversimplified approximation to the Witch of Agnesi shape or it may be regarded as a reasonable approximation to the wave shape produced by a special kind of roller*. See Figure 12.

The subscript "k" will be used to denote quantities evaluated in the compressed region (i.e. $0 < |z| < \frac{S}{2}$) of the square wave [e.g., $\epsilon = 2 \cdot B_k$].

Then, using Eq. (3.29), with h = 2.0, the integral expressions for $\overline{AB}$, F°, and G° given by Eqs. (3.25), (3.26), and (3.27) become simple algebraic expressions:

---

* Note: this special type of roller was suggested to me by Prof. Ascher H. Shapiro in a private communication on 6 September 1969.

$$\overline{AB} = \left\{ \frac{S \cdot (AB)_k + (L-S)}{L} \right\} = \left\{ 1 - \left(\frac{S}{L} \right) \cdot \left[1 - (AB)_k \right] \right\} \tag{3.30}$$

$$F^\circ = \left[S \cdot \left(\frac{A^2+B^2}{A^3B^3} \right)_k + (L-S) \right] \tag{3.31}$$

$$G^\circ = \left[S \cdot \left(\frac{A^2+B^2}{A^2B^2} \right)_k + (L-S) \right] \tag{3.32}$$

Substituting Eqs. (3.30), (3.31), and (3.32) into Eq. (3.28) gives:

$$\left(\frac{\bar{Q}}{\pi \bar{R}^2 c} \right) = \left\{ \frac{-\delta p_\lambda}{(\mu c/R)} \cdot \left(\frac{1}{4S \cdot \left[\left(\frac{A^2+B^2}{A^3B^3} \right)_k + \left(\frac{L}{S} - 1 \right) \right]} \right) + \frac{\left(1 - \frac{S}{L} \right) \left[\left(\frac{A^2+B^2}{A^3B^3} \right)_k - \left(\frac{A^2+B^2}{A^2B^2} \right)_k + \left(1 - (AB)_k \right) \right]}{\left[\left(\frac{A^2+B^2}{A^3B^3} \right)_k + \left(\frac{L}{S} - 1 \right) \right]} \right\} \tag{3.33}$$

Eq. (3.33) is the general relation between $\bar{Q}$ and δp_λ for a square wave shape; Eq. (3.33) is subject to the same restrictions as Eq. (3.28).

If two additional assumptions are now made, that:

$$B_k = \frac{\epsilon}{2} << 1 \tag{3.34}$$

which is a reasonable assumption, since roller pumps are usually operated in the nearly occlusive mode, and that:

$$\left(\frac{L}{S}\right) << \left(\frac{A^2+B^2}{A^3B^3}\right)_k \tag{3.35}$$

and observing that Eq. (2.9), with Eq. (3.34), implies that:

$$A_k \cong \frac{\pi}{2} \tag{3.36}$$

then Eq. (3.33) becomes:

$$\left(\frac{\bar{Q}}{\pi R^2 c}\right) \cong \left[\frac{-\delta p_1 \cdot R}{\mu c} \cdot \frac{\pi}{64} \cdot \frac{\epsilon^3}{S} + \left(1-\frac{S}{L}\right)\cdot\left(1-\frac{\pi\epsilon}{4}\right)\right] \tag{3.37}$$

Eq. (3.37) is a special case of Eq. (3.33) and holds only when Eqs. (3.34) and (3.35) are satisfied. Eq. (3.35) is equivalent to the condition:

$$\left(\frac{\epsilon^3}{S}\right) << \frac{5}{L} \tag{3.38}$$

when Eq. (3.34) is satisfied. Eq. (3.38) is a condition which is met by almost any reasonable set of square-wave parameters; so, in effect, the only restriction on Eq. (3.37), beyond the restrictions on Eq. (3.33), is that Eq. (3.34) be satisfied.

D. Modified Witch of Agnesi Wave Shape

The simple square wave shape, Eq. (3.29), which finally yielded Eq. (3.37), has a serious limitation as an approximation to the Witch of Agnesi wave shape. The limitation lies in the fact that the square wave lacks wall curvature,

so that ϵ and S for the square wave (see Figure 11) are not directly comparable to ϵ and d for the Witch of Agnesi wave (see Figure 4.) In order to obtain analytic results which can be related to the Witch of Agnesi shape, it is necessary to use a wave shape which is analytically simpler than Eq. (2.19) but which retains the "most important" properties of the Witch of Agnesi shape. In a peristaltic pump, most of the pressure rise across the pump is due to viscous forces acting on the liquid within the highly compressed regions of the tube; this is the region directly beneath the roller where the wave shape is mainly influenced by the values of d and ϵ. Therefore, as far as the pumping characteristics are concerned, the "most important" properties of the Witch of Agnesi are shared with the osculating parabola, Eq. (2.20).

So, in terms of the osculating parabola, a "Modified Witch of Agnesi" wave shape can be defined:

$$\eta = \eta_{max}(z) = 2 \cdot B(z) = \begin{cases} \left(\frac{1}{2d} z^2 + \epsilon \right), & \text{for } |z| < \sqrt{2md} \\ h, & \text{for } \sqrt{2md} < |z| \leq L/2 \end{cases} \tag{3.39}$$

See Figure 13.

In the following analysis, h = 2.0. Eq. (3.39) has the properties:

$$\epsilon = \eta_{max}(0) \tag{3.40}$$

and

$$d = \text{radius of curvature of } \eta_{max}(\zeta) \text{ at } \zeta = 0. \tag{3.41}$$

Eqs. (3.40) and (3.41) are identical to Eqs. (2.15) and (2.16), respectively, for the Witch of Agnesi shape; therefore ϵ and d for the modified Witch of Agnesi wave are *directly* comparable to ϵ and d for the Witch of Agnesi wave.

The value of "m" in Eq. (3.39) is selected so that two conditions are satisfied:

$$A \cong \frac{\pi}{2}, \quad \text{for} \quad |\zeta| < \sqrt{2md} \quad \left(\text{i.e., for} \quad B < \frac{m+\epsilon}{2}\right) \tag{3.42}$$

and

$$\left(\frac{\epsilon}{m}\right) << 1 \tag{3.43}$$

From Eq. (2.9), it is seen that a suitable value for m is:

$$m = 0.4 \tag{3.44}$$

so long as ϵ is constrained to satisfy:

$$\epsilon < \sim 0.10 \tag{3.45}$$

If Eqs. (3.44) and (3.45) are satisfied, then Eqs. (3.42) and (3.43) are also satisfactorily satisfied.

A useful assumption is that:

$$L << \frac{3 \cdot 2^{1/2} \cdot d^{1/2}}{\epsilon^{5/2}} \tag{3.46}$$

which is satisfied for most reasonable values of L and d when Eq. (3.45) is satisfied.

Substituting Eq. (3.39) into Eqs. (3.25), (3.26), and (3.27), subject to the conditions of Eqs. (3.42), (3.43), and (3.46), and substituting the expressions thus obtained into Eq. (3.28), gives the following relation:

$$\left(\frac{\bar{Q}}{\pi R^2 c}\right) \cong \left\{\frac{-\delta p_\lambda}{(\mu c/R)} \cdot \left(\frac{\epsilon^{5/2}}{3 \cdot 2^{7/2} \cdot d^{1/2}}\right) + \left[1 - \frac{\sqrt{2md}}{L}\left(2 - \frac{\pi m}{6}\right)\right]\right. \tag{3.47}$$

Using Eq. (3.44), Eq. (3.47) becomes:

$$\left(\frac{\bar{Q}}{\pi R^2 c}\right) \cong \left\{\frac{-\delta p_\lambda}{(\mu c/R)} \cdot \left[\frac{\epsilon^{5/2}}{(33.9)\, d^{1/2}}\right] + \left[1 - (1.60)\frac{d^{1/2}}{L}\right]\right\} \tag{3.48}$$

Eqs. (3.47) and (3.48) are valid only for tubes which are circular in cross-section when not squeezed.

The most significant feature of Eq. (3.47) is that the coefficient of $\left(\frac{\delta p_\lambda}{(\mu c/R)}\right)$ *is independent of* m *and* L. This says that the contribution of δp_λ to $\bar{Q}$ is dependent upon the geometry

near the origin (z = 0), i.e., upon ϵ and d, but is not dependent upon the geometry elsewhere, i.e., upon m and L.

If Eqs. (3.42), (3.43), and (3.46) are satisfied, then the coefficient of $(\frac{\delta p_s}{\mu c/R})$ in Eq. (3.47) should be very nearly equal to $(\frac{1}{4F^\circ})$ in Eq. (3.28) for the Witch of Agnesi wave shape. That is, it should be true, for the Witch of Agnesi wave shape, Eq. (2.19) - subject to the constraints of Eqs. (3.45) and (3.46) - that

$$\frac{1}{4F^\circ} \cong \frac{\epsilon^{5/2}}{3 \cdot 2^{7/2} d^{1/2}} = \frac{\epsilon^{5/2}}{(33.9) \cdot d^{1/2}} \qquad (3.49)$$

Eq. (3.49) can be checked by numerically computing $(\frac{1}{4F^\circ})$, as outlined in Section 3.3B, for particular values of ϵ, d, L, and γ^*, with h = 2.0, and comparing the value thus obtained with the value given by Eq. (3.49). See Table 2.

4. BLOOD DAMAGE CHARACTERISTICS

4.1 Criteria for Index of Hemolysis

As discussed in the Introduction (Section 1.3), a convenient measure of blood damage is the Index of Hemolysis (I.H.) defined:

$$\text{I.H.} \equiv \left[\frac{\text{mg. Hb released into plasma}}{\text{100 ml. of blood pumped}}\right] \tag{4.1}$$

where Hb ≡ Hemoglobin (from ruptured red blood cells).

P. L. Blackshear, et al., on the basis of their own experiments and the experiments of other investigators, report[1] that the I.H. for blood flow through small-diameter tubes of circular cross-section is independent of the flow rate, Q, through the tubes. On the basis of other experiments, in which blood was subjected to high turbulent shears far from any solid surfaces, Blackshear, et al., report[1] that blood can withstand very high shear rates ($\sim 10^6$/sec) without hemolysis when walls are absent; such is not the case when walls are nearby. They conclude that the hemolysis which occurs when blood flows through tubes at moderate shear rates is a wall-related phenomenon. The data which they report for hemolysis in tubes is shown in Figure 14. In this figure, points 5 and 6 merely confirm that, in a given experiment with the tube radius fixed, I.H. is independent of flow rate. Points 1, 2, 3, and 4 indicate that I.H. is approximately proportional to a reciprocal power of the tube radius, R_T:

$$I.H. \propto \sim\left(\frac{1}{R_T^2}\right) \quad \text{or} \quad \sim\left(\frac{1}{R_T^3}\right) \tag{4.2}$$

Blackshear, et al., obtained the relation

$$I.H. \propto \left(\frac{1}{R_T^3}\right) \tag{4.3}$$

from the following arguments. There is a diffusion flux of red cells toward the wall. A certain fraction of the red cells which reach the wall are hemolyzed. The flux is characterized by a "diffusion" coefficient, D; this coefficient, D, is assumed to be proportional to the average shear rate in the flow, in order to satisfy the requirement that the I.H. be independent of the volume flow rate. In fact these arguments imply that the rate of hemolysis is proportional to the product of the average shear rate and the wall area and should yield

$$I.H. \propto \left(\frac{1}{R_T^2}\right) \tag{4.4}$$

rather than Eq. (4.3).

It is interesting to note that Eq. (4.4) may also be obtained from different physical arguments which are as follows:

(i) Red-cell destruction (i.e., hemolysis) takes place at the wall.

(ii) Because of (i), the amount of hemolysis (mg of Hb released) should be directly proportional to the wall area, i.e., to the product of the wall perimeter ($2\pi R_T$) and the tube length (λ).

(iii) I.H., being the number of mg of Hb released *per 100 ml of blood pumped*, should be inversely proportional to the volume flow rate (Q) of blood through the tube, other things being equal.

(iv) The amount of red-cell destruction (mg of Hb released) at the wall should be directly proportional to the absolute value of the shear stress at the wall ($|\tau_{wall}|$).

A mechanism which could account for -- i.e., make plausible -- point (iv) above, is the following: red cells are known to adhere to foreign surfaces. If a red cell is

"ripped off" of a surface to which it has adhered, then the membrane of the red cell is likely to be ruptured and Hb released into the plasma. The likelihood of a red cell, adhering to the wall of a tube, being "ripped off" of the wall, should be proportional to the absolute value of the velocity of fluid near the wall, i.e., proportional to the absolute value of the shear stress at the wall ($|\tau_{wall}|$).

Assuming that the preceding argument [points (i) through (iv)] is correct, then the following result is obtained:

$$I.H. = \frac{k^* \cdot (2\pi R_T) \cdot |\tau_{wall}| \cdot \lambda}{Q} \tag{4.5}$$

where k* is a "constant" of proportionality which could be a function of blood fragility, temperature, hematocrit, wall roughness, chemical composition of the wall, etc.

For a steady, fully-developed flow through a straight tube of circular cross-section and radius, R_T, the relevant flow quantities are[14]:

$$W(r) = \frac{R_T^2}{4\mu} \cdot \frac{dp}{dZ} \cdot \left(1 - \frac{r^2}{R_T^2}\right) \tag{4.6}$$

where W ≡ longitudinal velocity

r ≡ radial coordinate

$$|\tau_{wall}| = \left| \mu \left(\frac{\partial W}{\partial r}\right)_{r=R_T} \right| = \frac{R_T}{2} \cdot \frac{dp}{dZ} \tag{4.7}$$

$$Q = \frac{\pi R_T^4}{8\mu} \cdot \frac{dp}{dZ} \tag{4.8}$$

Substituting Eqs. (4.7) and (4.8) into Eq. (4.5) gives:

$$I.H = \left[\frac{k^* \cdot 8\mu\lambda}{R_T^2}\right]$$

which has the form of Eq. (4.4).

Eq. (4.5), which applies only to the case of a right circular cylindrical tube, can be generalized to the case of a constant-perimeter tube having variable elliptic cross-sectional shapes, a wave-length λ, and a time mean flow $\bar{Q}$. This generalization would be applicable to the model of a peristaltic pump developed in this paper.

The generalized version of Eq. (4.5) is:

$$I.H. = \left[\frac{k^* \cdot (2\pi R) \cdot \int_0^\lambda |(\tau_{wall})_{average}| \cdot dz}{\bar{Q}}\right] \tag{4.9}$$

where $|(\tau_{wall})_{average}|$ is the absolute value of the average (mean) shear stress on the wall of the tube at a particular transverse cross-section in the wave frame.

Before proceeding any further with Eq. (4.9), it is necessary to find analytic expressions for (τ_{wall}) and for $[(\tau_{wall})_{average}]$.

4.2 Shear Stress on the Wall of the Tube

A. Shear Stress Distribution on the Wall of an Elliptical Cross-Section

In Section 3.2 it was assumed that transverse components of velocity were negligible. The ultimate result of that assumption was Eq. (3.6) for the dimensionless longitudinal velocity in the wave frame. Once again making that same assumption, and also assuming that the shear forces due to the transverse components of velocity are negligible, it follows then that the shear stress, τ, at the wall is:

$$\tau_{wall} = -\mu \left.\frac{\partial w}{\partial n}\right|_{wall} = -\mu (\nabla w)\Big|_{wall} \cdot \underset{\sim}{n} \tag{4.10}$$

where n is the local coordinate in the direction of $\underset{\sim}{n}$, the unit inner normal vector to the wall.

In Appendix 3 it is shown that Eq. (4.10), with the velocity distribution given in Eq. (3.6) and with the wall shape given by Eq. (2.3), becomes:

$$\left[\frac{-\tau_{wall}}{(4\mu c/R)}\right] = \left[\frac{F}{AB} + 1\right] \cdot \left[\frac{\xi^2}{A^2}\left(\frac{1}{A^2} - \frac{1}{B^2}\right) + \frac{1}{B^2}\right]^{1/2} \tag{4.11}$$

where

$$F \equiv \left(\frac{q}{\pi R^2 c}\right) \tag{4.12}$$

and where

$$-A \leq \xi \leq +A$$

B. Maximum Shear Stress on the Wall of an Elliptical Cross-Section

Differentiation of Eq. (4.11) with respect to ξ indicates that an extremum of $\frac{-\tau_{wall}}{4\mu c/R}$ occurs at $\xi = 0$ [i.e., the extremum occurs at $(\xi,\eta) = (0,0)$ or at $(0,2B)$]:

$$\left[\frac{-\tau_{wall}}{4\mu c/R}\right]\Bigg|_{\xi=0} = \left(\frac{F}{AB} + 1\right)\cdot\frac{1}{B} \tag{4.13}$$

A consideration of the second derivative of τ_{wall} with respect to ξ shows that Eq. (4.13) is a *minimum* extremum when

$$\left[\frac{F}{AB} + 1\right] < 0 \tag{4.14a}$$

and is a *maximum* extremum when

$$\left[\frac{F}{AB} + 1\right] > 0 \tag{4.14b}$$

Eq. (4.13) is plotted, for various values of F, in Figure 15. Figure 16 shows how τ_{wall} at $\xi = 0$ varies longitudinally along a particular wave shape. A significant feature of Figure 16 is that $|\tau_{wall}|_{\xi=0}$ has finite local maxima at $\gamma = 0$ and at a non-zero value of γ.

C. Average Shear Stress on the Wall of an Elliptical Cross-Section

The average shear stress (non-dimensionalized) is:

$$\left[\frac{-\tau_{wall}}{4\mu c/R}\right]_{average} \equiv \frac{1}{2\pi R}\cdot\int_0^{2\pi R}\left(\frac{-\tau_{wall}}{4\mu c/R}\right)dS \tag{4.15}$$

where

dS = differential arc length on wall of elliptical cross-section

$$= \left[(dx)^2 + (dy)^2\right]^{1/2}_{wall} = \left[1 + \left(\frac{dy}{dx}\right)^2\right]^{1/2}_{wall} dx \tag{4.16}$$

Solving Eqs. (2.3) and (2.11) for y, differentiating to get $\left(\frac{dy}{dx}\right)\Big|_{wall}$, and substituting into Eq. (4.16) gives:

$$dS = \left[\frac{a^2 - x^2(1 - b^2/a^2)}{a^2 - x^2}\right]^{1/2} dx \tag{4.17}$$

Substituting Eqs. (4.17) and (4.11) into Eq. (4.15), and using Eqs. (2.12) and (2.6) gives:

$$\left(\frac{-\tau_{wall}}{4\mu c/R}\right)_{average} = \frac{4}{2\pi R}\int_0^a \left(\frac{F}{AB} + 1\right)\cdot\left[\frac{x^2}{a^2}\left(\frac{1}{A^2} - \frac{1}{B^2}\right) + \frac{1}{B^2}\right]^{1/2}\cdot \cdot\left[\frac{a^2 - x^2(1 - b^2/a^2)}{a^2 - x^2}\right]^{1/2} dx \tag{4.18}$$

Now make the substitutions into Eq. (4.18):

$$x = RAu \quad ; \quad dx = RA\,du \; ; \quad a = RA \tag{4.19}$$

and use the new limits of integration:

$$\begin{aligned} u &= 1 \quad \text{when } x = a \\ u &= 0 \quad \text{when } x = 0 \end{aligned} \tag{4.20}$$

With substitutions (4.19) and (4.20), Eq. (4.18) becomes:

$$\left(\frac{-\tau_{wall}}{4\mu c/R}\right)_{average} = \left(\frac{F}{AB} + 1\right)\cdot K(B,A) \tag{4.21}$$

where

$$K(B,A) \equiv \frac{2}{\pi} \cdot \frac{A}{B} \cdot \int_0^1 \frac{\left[1 - u^2\left(1 - B^2/A^2\right)\right]}{\left[1 - u^2\right]^{1/2}} \cdot du \qquad (4.22)$$

Eq. (4.22), subject to the constant perimeter condition of Eq. (2.8), is plotted in Figure 17. Eq. (4.21), subject to Eq. (2.8) is plotted in Figure 18 for various values of F. Also plotted in the same figure are comparison plots of Eq. (4.13).

NOTE: Eq. (4.21) is an approximation to the actual average shear stress on the tube wall at any given cross-section. Only the longitudinal component of velocity, w, is known (itself approximately), so only the component of shear force due to w can be determined. The averaging performed in Eq. (4.15) does *not* introduce any new errors or approximations into the analysis. Any errors or approximations in Eq. (4.21) are already implicitly present in Eq. (4.11).

4.3 Index of Hemolysis for Square Wave Shape

Using Eqs. (4.9), (2.12) and (3.20), the relation for I.H. can be expressed:

$$I.H. = \frac{k^* \cdot 2\pi R^2}{\bar{Q}} \cdot \int_0^L \left|(\tau_{wall})_{average}\right| dz \qquad (4.23)$$

$(\tau_{wall})_{average}$ is given by Eqs. (4.21) and (4.22). It should be noted, with regard to Eq. (4.22), that

$$K(1,1) = 1 \qquad (4.24)$$

and, when $B << 1$ and $A \cong \frac{\pi}{2}$, that:

$$K(B, \tfrac{\pi}{2}) \cong \frac{\pi}{4B} \tag{4.25}$$

Then, for the geometry of the square wave, defined by Eq. (3.29) and diagramed in Figure 11, with h = 2.0, Eq. (4.23) becomes:

$$I.H. = \frac{k^* \cdot 2\pi R^2}{\bar{Q}} \left\{ S \cdot \left| (\tau_{wall})_{average} \right|_k + (L-S) \cdot \left| (\tau_{wall})_{aver.} \right|_{\substack{A=1 \\ B=1}} \right\} \tag{4.26}$$

where the subscript "k" denotes a quantity evaluated in the compressed region of the square wave.

Now assume that

$$B_k = \frac{\epsilon}{2} << 1 \tag{4.27}$$

Then, by Eqs. (4.21), (4.22), and (4.25) and using Eq. (2.9):

$$\left| (\tau_{wall})_{average} \right|_k \cong \frac{2\mu c}{R} \cdot \frac{\pi}{\epsilon} \cdot \left| \frac{4F}{\pi\epsilon} + 1 \right| \tag{4.28}$$

By Eqs. (4.21), (4.22), and (4.24):

$$\left| (\tau_{wall})_{average} \right|_{\substack{A=1 \\ B=1}} = \frac{4\mu c}{R} \cdot \left| F + 1 \right| \tag{4.29}$$

Using Eqs. (4.28) and (4.29), Eq. (4.26) becomes

$$I.H. \cong \frac{k^* \cdot \pi \cdot 4\mu c R}{\bar{Q}} \left\{ \frac{\pi S}{\epsilon} \cdot \left| \frac{4F}{\pi\epsilon} + 1 \right| + 2(L-S) \left| F + 1 \right| \right\} \tag{4.30}$$

But from Eqs. (3.24) and (4.12):

$$F = \left(\frac{\bar{Q}}{\pi R^2 c} - \overline{AB} \right) \tag{4.31}$$

and, from Eq. (3.30) for the square wave, using Eqs. (2.9) and (4.27):

$$\overline{AB} \cong \left[1 - \frac{S}{L} + \frac{\epsilon \pi}{4} \cdot \frac{S}{L} \right] \tag{4.32}$$

So, substituting Eq. (3.37) [which is valid for the square wave when Eqs. (3.34) and (3.38) are true] and Eq. (4.32) into Eq. (4.31) gives:

$$F \cong \left[\frac{-\delta p_\lambda \cdot R}{\mu c} \cdot \frac{\pi}{64} \cdot \frac{\epsilon^3}{S} - \frac{\pi \epsilon}{4} \right] \tag{4.33}$$

Substituting Eq. (4.33) into (4.30) gives:

$$I.H. \cong \frac{k^* 4\pi \mu c R}{\bar{Q}} \left\{ \frac{\delta p_\lambda \cdot R}{\mu c} \cdot \frac{\pi}{16} \cdot \epsilon + 2 \cdot (L - S) \cdot \left| \frac{-\delta p_\lambda \cdot R}{\mu c} \cdot \frac{\pi}{64} \cdot \frac{\epsilon^3}{S} - \frac{\pi \epsilon}{4} + 1 \right| \right\} \tag{4.34}$$

Then, assuming

$$\epsilon << 1 \tag{4.35}$$

and assuming

$$\left(\frac{L-S}{S}\right)\epsilon^2 << 1 \tag{4.36}$$

Eq. (4.34) becomes:

$$I.H. \cong \frac{k^* \cdot 4\pi\mu c R}{\bar{Q}} \left\{ \frac{\delta p_\lambda \cdot R}{\mu c} \cdot \frac{\pi\epsilon}{16} + 2\cdot(L-S) \right\} \tag{4.37}$$

Eq. (4.37) is the relation for I.H. for the square wave shape, subject to the assumptions of Eqs. (4.35) and (4.36).

4.4 Index of Hemolysis for Modified Witch of Agnesi Wave Shape

The I.H. for the modified Witch of Agnesi wave shape can be determined by using Eq. (4.23) in conjunction with Eqs. (4.21), (4.22), (3.39) and (2.9). Assuming that Eqs. (3.44) and (3.45) are valid, then Eq. (2.9) becomes equivalent to Eq. (3.42). Eqs. (3.27) and (3.26) then become, respectively

$$G^0 \cong \frac{\pi \cdot 2^{3/2} d^{1/2}}{\epsilon^{3/2}} \left[1 + \frac{2\epsilon}{3\pi m} \right] \tag{4.38}$$

and

$$F^0 \cong \frac{3 \cdot 2^{3/2} d^{1/2}}{\epsilon^{5/2}} \left[1 + \frac{2\epsilon}{3\pi m} \right] \tag{4.39}$$

where it has been assumed that

$$\left(\frac{\epsilon}{m}\right)^{3/2} << 1 \tag{4.40}$$

and

$$L << \left(\frac{2^{1/2}\pi d^{1/2}}{\epsilon^{3/2}}\right) \tag{4.41}$$

From Eqs. (4.21) and (4.22), with Eqs. (3.42), (4.25), and (3.39), it follows that

$$\left|\left[(\tau_{wall})_{average}\right]_k\right| \cong \frac{4\mu c}{R}\cdot|r| \tag{4.42}$$

where

$$r \equiv \left[\frac{8d^2F}{(\eta^2+2\epsilon d)^2} + \frac{\pi d}{(\eta^2+2\epsilon d)}\right] \tag{4.43}$$

and where the subscript "k" denotes a quantity which is to be evaluated in the compressed region of the modified Witch of Agnesi wave shape (i.e., in the region defined by

$$|\eta| < \sqrt{2md}\ )$$

Then, for this wave shape, Eq. (4.23) becomes:

$$I.H. \cong \frac{(16)k^*\pi\mu cR}{\bar{Q}}\cdot\left\{\int_0^{\sqrt{2md}}|r|\,d\eta + \left|F+1\right|\cdot\left[\frac{L}{2}-\sqrt{2md}\right]\right\} \tag{4.44}$$

Now, using the assumption of Eq. (3.43) and making the additional assumption:

$$|F+1| = (F+1) \tag{4.45}$$

then it can be shown (see Appendix 4) that Eq. (4.44) becomes:

$$\begin{aligned} I.H \cong \frac{(16)\pi k^* \mu c R}{\bar{Q}} \cdot \Bigg\{ & \frac{\pi^2 d^{1/2}}{3 \cdot 2^{3/2} \epsilon^{1/2}} \cdot \left[2 - \frac{\delta p_\lambda \cdot R}{\mu c} \cdot \frac{\epsilon^{3/2}}{\pi 2^{3/2} d^{1/2}} \right] \cdot \\ & \cdot \left[\frac{1}{2} - \frac{2}{\pi} \tan^{-1} \left(\frac{1}{3^{1/2}} \left[1 + \frac{\delta p_\lambda \cdot R}{\mu c} \cdot \frac{\epsilon^{3/2}}{\pi 2^{3/2} d^{1/2}} \right]^{1/2} \right) \right] \\ & + \frac{\pi d^{1/2}}{2^{1/2} 3^{1/2} \epsilon^{1/2}} \left[1 + \frac{\delta p_\lambda \cdot R}{\mu c} \cdot \frac{\epsilon^{3/2}}{\pi 2^{3/2} d^{1/2}} \right]^{1/2} \\ & + \left[\frac{-\pi d^{1/2}}{2^{1/2} m^{1/2}} + \frac{L}{2} - 2^{1/2} m^{1/2} d^{1/2} \right] \Bigg\} \end{aligned} \tag{4.46}$$

It can be shown (see Appendix 5) that, *if*

$$\epsilon_0 \equiv \left[\pi^{2/3} 2^{5/3} d^{1/3} \left(\frac{\mu c}{\delta p_\lambda \cdot R} \right)^{2/3} \right] << 1 \tag{4.47}$$

then I.H., as given by Eq. (4.46) has a *minimum* value at $\epsilon = \epsilon_0$.

A "typical" set of parameters is:

$$\begin{aligned} \delta p_\lambda &= 1.5 \times 10^5 \text{ gm/cm sec}^2 \ (= 112.5 \text{ mm Hg}) \\ R &= 1.0 \text{ cm} \\ c &= 26.5 \text{ cm/sec} \\ \mu &= 0.05 \text{ gm/cm sec} \\ d &= 4.0 \end{aligned} \tag{4.48}$$

Using the parameters of Eq. (4.48), Eq. (4.47) gives the value:

$$\epsilon_o = 4.62 \times 10^{-3} \tag{4.49}$$

which satisfies the inequality of Eq. (4.47).

From Eq. (4.47) it follows that

$$\left(\frac{\delta p_\lambda \cdot R}{\mu c} \cdot \frac{\epsilon^{3/2}}{\pi 2^{3/2} d^{1/2}}\right) \equiv 2\left(\frac{\epsilon}{\epsilon_o}\right)^{3/2} \tag{4.50}$$

Substituting Eq. (4.50) into Eq. (4.46) gives

$$\begin{aligned} I.H. \cong \frac{(16)\pi k^* \mu c R}{\bar{Q}} \Bigg\{ & \frac{\pi^2 d^{1/2}}{3 \cdot 2^{1/2} \epsilon^{1/2}} \cdot \left[1 - \left(\frac{\epsilon}{\epsilon_o}\right)^{3/2}\right] \cdot \\ & \cdot \left[\frac{1}{2} - \frac{2}{\pi} \tan^{-1}\left\{\frac{1}{3^{1/2}}\left[1 + 2\left(\frac{\epsilon}{\epsilon_o}\right)^{3/2}\right]^{1/2}\right\}\right] \\ & + \frac{\pi d^{1/2}}{2^{1/2} 3^{1/2} \epsilon^{1/2}} \cdot \left[1 + 2\left(\frac{\epsilon}{\epsilon_o}\right)^{3/2}\right]^{1/2} \\ & + \left[\frac{-\pi d^{1/2}}{2^{1/2} m^{1/2}} + \frac{L}{2} - 2^{1/2} m^{1/2} d^{1/2}\right] \Bigg\} \end{aligned} \tag{4.51}$$

The right hand side of Eq. (4.51) is grouped into three terms. The first of these terms is positive semidefinite (it equals zero only when $(\epsilon/\epsilon_0) = 1$); the second term is positive definite; the third term may be either positive or negative (though if L is sufficiently large, the term will be positive), but since it is much smaller in magnitude than the second term (because Eq. (3.43) must be satisfied) it cannot influence the sign of I.H. Therefore, I.H., as given by Eq. (4.51), is positive definite, as required by Eq. (4.9).

If ϵ in Eq. (3.47) is set equal to ϵ_0 (as given by Eq. (4.47)), then Eq. (3.47) becomes:

$$\frac{\bar{Q}(\epsilon=\epsilon_o)}{\pi R^2 c} \cong \left\{ \frac{-\pi\epsilon_o}{6} + \left[1 - \frac{\sqrt{2md}}{L}\left(2 - \frac{\pi m}{6}\right)\right]\right\} \tag{4.52}$$

So, when the inequality of Eq. (4.47) is satisfied, and when

$$\left(\frac{d^{1/2}}{L}\right) << 1 \tag{4.53}$$

then Eq. (4.52) gives, approximately:

$$\bar{Q}(\epsilon=\epsilon_o) \cong \pi R^2 c \tag{4.54}$$

Substituting ϵ_0 for ϵ in Eq. (4.51), using Eq. (4.47), neglecting the (small) third term of Eq. (4.51), and eliminating c by using Eq. (4.54), gives:

$$I.H.(\epsilon=\epsilon_o) \cong 2^{8/3}\pi k^* \left(\frac{\delta p_\lambda \cdot d \cdot \mu^2}{\bar{Q}}\right)^{1/3} \tag{4.55}$$

Eq. (4.55) is an approximate expression for the minimum value of I.H. obtainable for given values of δp_λ, d, and $\bar{Q}$, for the modified Witch of Agnesi wave shape. For the "typical" set of parameters given in Eq. (4.48), Eq. (4.55) becomes

$$I.H.\ (\epsilon = \epsilon_0 = 4.62 \times 10^{-3}) = (16.67 \frac{gm}{cm^2 sec}) \cdot k^* \tag{4.56}$$

The appearance of m in a term [e.g., in certain terms of Eqs. (4.46), (4.51), and (4.52)] indicates that details

of the wave shape, other than ϵ and d, are significant for that term, so that the modified Witch of Agnesi wave shape (Figure 13) is not an accurate approximation to the regular Witch of Agnesi wave shape (Figure 4) *for that term*. Terms (and expressions) not involving m are, however, well-approximated and should be the same for both the modified and regular Witch of Agnesi wave shapes.

Eqs. (4.46), (4.47), (4.51), and (4.55) indicate that, for the Witch of Agnesi wave shape, I.H. at first decreases as ϵ decreases, then passes through a minimum value at $\epsilon = \epsilon_0$, and then increases indefinitely as ϵ decreases further. This behavior of I.H. is to be contrasted with that for the square wave shape. Eq. (4.37) indicates that, for the square wave, I.H. decreases linearly with ϵ until it becomes equal to a finite value when $\epsilon = 0$.

In order to make an additional comparison between the expressions for I.H. for the square and Witch of Agnesi wave shapes, it is necessary to express d for the Witch of Agnesi wave in terms of S for the square wave. Figures 11 and 13 suggest that an appropriate relation between d and S is:

$$d^{1/2} \sim S \tag{4.57}$$

Eq. (4.57) is, of course, only a crude approximation. Substituting Eq. (4.57) into Eq. (4.47) gives an expression for a quantity which will be designated $\epsilon_0(S)$; then letting $\epsilon = \epsilon_0(S)$ in Eq. (4.37), neglecting the term involving the factor (L - S), and using Eq. (4.54) to eliminate c, yields

$$I.H. \sim \frac{k^* \pi^2}{2^{1/3}} \left(\frac{\delta p_\lambda S^2 \mu^2}{\bar{Q}} \right)^{1/3} \qquad (4.58)$$

Eq. (4.58), while only a crude approximation to I.H. for the square wave shape when $\epsilon = \epsilon_0(S)$, nonetheless reveals, when compared with Eq. (4.55) for the Witch of Agnesi shape, that the I.H. for the square shape has a functional dependence upon δp_λ, μ, and $\bar{Q}$ which is similar to that of the Witch of Agnesi shape -- when $\epsilon \cong \epsilon_0 \sim \epsilon_0(S)$. Therefore, when operating in the vicinity of $\epsilon = \epsilon_0$ (for the Witch of Agnesi) or $\epsilon = \epsilon_0(S)$ (for the square wave), neither the square nor the Witch of Agnesi shapes should enjoy any particular advantage over the other shape with regard to the functional character of the dependence of I.H. upon δp_λ, μ, and $\bar{Q}$; a relative advantage may exist, of course, in the absolute magnitude of I.H., but an advantage will not exist in the type of functional dependence.

5. NECESSARY CONDITIONS FOR VALIDITY OF THEORY

5.1 Inertia-Free Flow

A. Condition for Inertia-Free Flow

The validity of the theory presented in the preceding sections is dependent upon the validity of the assumption made in Section 3.2, that the flow is inertia-free - permitting the longitudinal Navier-Stokes equation to be approximated by Eq. (3.1). The full longitudinal Navier-Stokes equation for steady flow of a Newtonian fluid in the wave frame is:

$$u\frac{\partial w}{\partial x} + v\frac{\partial w}{\partial y} + w\frac{\partial w}{\partial z} = \frac{-1}{\rho}\frac{\partial p}{\partial z} + \nu\left(\frac{\partial^2 w}{\partial x^2} + \frac{\partial^2 w}{\partial y^2} + \frac{\partial^2 w}{\partial z^2}\right) \tag{5.1}$$

where $\nu \equiv \mu/\rho \equiv$ kinematic viscosity of the fluid. The inertia terms (i.e., the left hand side) of Eq. (5.1) may be neglected relative to the viscous terms (on the right hand side) if

$$\left|\frac{u\frac{\partial w}{\partial x} + v\frac{\partial w}{\partial y} + w\frac{\partial w}{\partial z}}{\nu\left[\frac{\partial^2 w}{\partial x^2} + \frac{\partial^2 w}{\partial y^2} + \frac{\partial^2 w}{\partial z^2}\right]}\right| << 1 \tag{5.2}$$

An order of magnitude analysis shows that the numerator of the left hand side of Eq. (5.2) is of the order of its third term, $w\frac{\partial w}{\partial z}$: From Figure 20:

The characteristic time is the period required for a typical fluid particle at the wall to pass from a point immediately in front of the roller to a point directly beneath the roller. Therefore:

$$\text{Characteristic time} \equiv \tau \sim \frac{d \cdot R}{c} \tag{5.3}$$

and it follows that the characteristic velocities are:

$$V = v \sim R/\tau \sim c/d \tag{5.4}$$

$$U = u \sim R/\tau \sim c/d \tag{5.5}$$

$$\text{Waveframe longitudinal centerline velocity} \equiv w_o \tag{5.6}$$

$$\text{Waveframe longitudinal velocity at wall} \equiv -c \tag{5.7}$$

Characteristic lengths for variations in longitudinal velocity in the compressed region of the tube:

$$\Delta x \sim R \tag{5.8}$$

$$\Delta y \sim \epsilon \cdot R \tag{5.9}$$

$$\text{Typical longitudinal waveframe velocity} = w \sim (w_o + c) \tag{5.10}$$

Then using Eqs. (5.6), (5.7), and (5.8):

$$\frac{\partial w}{\partial x} \sim \left(\frac{w_o + c}{R} \right) \tag{5.11}$$

and using Eqs. (5.6), (5.7), and (5.9):

$$\frac{\partial w}{\partial y} \sim \left(\frac{w_o + c}{\epsilon \cdot R}\right) \tag{5.12}$$

But, by the continuity equation

$$\frac{\partial w}{\partial z} = \left(-\frac{\partial u}{\partial x} - \frac{\partial v}{\partial y}\right) \tag{5.13}$$

Then, using Eqs. (5.5) and (5.8):

$$\frac{\partial u}{\partial x} \sim \left(\frac{c}{d \cdot R}\right) \tag{5.14}$$

and, using Eqs. (5.4) and (5.9):

$$\frac{\partial v}{\partial y} \sim \left(\frac{c}{\epsilon d R}\right) \tag{5.15}$$

Substituting Eqs. (5.14) and (5.15) into (5.13) gives, when ϵ is small:

$$\frac{\partial w}{\partial z} \sim \left(\frac{c}{\epsilon d R}\right) \tag{5.15b}$$

Collecting terms, and keeping only the largest term, gives the numerator of Eq. (5.2):

$$\left(u\frac{\partial w}{\partial x} + v\frac{\partial w}{\partial y} + w\frac{\partial w}{\partial z}\right) \sim \frac{c(w_o + c)}{\epsilon d R} \sim w\frac{\partial w}{\partial z} \tag{5.16}$$

Therefore the sum of the three inertial terms is of the same

order of magnitude as $w \frac{\partial w}{\partial z}$.

B. Calculation of the Reynolds Number

The absolute value of the ratio of the inertia terms to the viscous terms, at any point in the fluid, is designated as the Reynolds number at that point. The complete Reynolds number is given by the left hand side of Eq. (5.2). But, by using Eq. (5.16) and by using the assumption that:

$$\left| \frac{\partial^2 w}{\partial z^2} \right| << \left| \frac{\partial^2 w}{\partial x^2} + \frac{\partial^2 w}{\partial y^2} \right| \tag{5.17}$$

it is possible to define an approximate Reynolds number, Re, which is sufficiently simple to make analytic computations possible:

$$Re \equiv \left| \frac{w \frac{\partial w}{\partial z}}{\nu \left(\frac{\partial^2 w}{\partial x^2} + \frac{\partial^2 w}{\partial y^2} \right)} \right| \tag{5.18}$$

Using Eqs. (3.5) and (2.12), Eq. (5.18) becomes:

$$\left(\frac{Re}{Rc/\nu} \right) = \left| \frac{\omega \frac{\partial \omega}{\partial \zeta}}{\frac{\partial^2 \omega}{\partial \xi^2} + \frac{\partial^2 \omega}{\partial \eta^2}} \right| \tag{5.19}$$

The approximate criterion for inertia-free flow is that Re satisfy:

$$Re << 1 \tag{5.20}$$

at every point in the flow, or equivalently, that the *maximum* Reynolds number in the flow, Re**, satisfy:

$$Re^{**} << 1 \tag{5.21}$$

Substituting Eqs. (3.15) and (3.18) into Eq. (3.6) gives:

$$\omega = \left\{-1 + 2\left[\frac{F}{AB} + 1\right]\cdot\left[1 - \frac{\xi^2}{A^2} - \frac{(\eta-B)^2}{B^2}\right]\right\} \tag{5.22}$$

From Eq. (5.22), straightforward calculation yields on the centerline:

$$\left(\omega \frac{\partial \omega}{\partial \gamma}\right)_{\substack{\xi=0 \\ \eta=B}} = \left\{-2 \frac{dB}{d\gamma}\left(\frac{1}{A}\frac{dA}{dB} + \frac{1}{B}\right)\left(\frac{F}{AB}\right)\cdot\left(\frac{2F}{AB} + 1\right)\right\} \tag{5.23}$$

The Reynolds number has its maximum value (on any arbitrary transverse cross-section) at a point close to the cross-sectional center, $(\xi,\eta) = (0,B)$. Substituting Eq. (5.22) into (5.19) and evaluating at the centerline gives:

$$\left(\frac{Re}{Rc/\nu}\right)_{\substack{\xi=0 \\ \eta=B}} = \left|\frac{\frac{dB}{d\gamma}\left[A + B\frac{dA}{dB}\right]\left[2F + AB\right]\cdot F}{2\left[A^2 + B^2\right]\left[F + AB\right]}\right| \tag{5.24}$$

It is now necessary to find the maximum of $\left(\frac{Re}{Rc/\nu}\right)_{\substack{\xi=0 \\ \eta=B}}$ with respect to γ.

Inspection of Eq. (5.24) shows that

$$\left(\frac{Re}{Rc/\nu}\right)_{\substack{\xi=0 \\ \eta=B}} \longrightarrow +\infty \quad , \text{ when } \quad AB \longrightarrow -F \tag{5.25}$$

This singularity in Re is due to the viscous terms going to zero. Before concluding that Eq. (5.25) says that the inertia forces are *important* when $AB \cong -F$, it is necessary to compare the magnitude of the inertia forces in this part of the flow with the magnitude of inertia forces elsewhere in the flow.

When

$$AB \cong (-F) << 1 \tag{5.26}$$

then

$$B \cong \frac{-F}{A} << 1 \tag{5.27}$$

and, by Eq. (2.9)

$$A \cong \frac{\pi}{2} - \alpha \cdot B^2 \cong \frac{\pi}{2} \quad , \quad (\alpha \sim 1.) \tag{5.28}$$

(the inequality of (5.26) is true for small ϵ and "typical" values of δp_λ and other parameters.)

So, substituting Eq. (5.28) into (5.27) gives:

$$B \cong \frac{-2F}{\pi} \tag{5.29}$$

then, using Eqs. (5.28) and (5.29):

$$\frac{dA}{dB} \cong -2 \cdot \alpha \cdot B \cong \frac{4F\alpha}{\pi} \quad , \quad (\alpha \sim 1.) \tag{5.30}$$

Substituting Eqs. (5.28), (5.29), and (5.30) into Eq. (5.23), and using the inequality of Eq. (5.26), then gives:

$$\left(\omega\frac{\partial\omega}{\partial\eta}\right)_{\substack{\xi=0\\ \eta=B}} \cong \frac{\pi}{F}\left(\frac{dB}{d\eta}\right) \qquad \text{, when } AB = -F \ll 1 \tag{5.31}$$

Then, using Eqs. (3.39), (5.28), and (5.26) to eliminate F and B, Eq. (5.31) becomes:

$$\left(\omega\frac{\partial\omega}{\partial\eta}\right)_{\substack{\xi=0\\ \eta=B}} = \left(\frac{-4\eta}{\eta^2+2\epsilon d}\right)$$

$$= 0, \text{ if } \eta = 0 \tag{5.32}$$

$$\to 0, \text{ as } \eta \to \infty$$

From Eq. (5.32) it can be shown that the maximum value of Eq. (5.32) is:

$$\left|\left(\omega\frac{\partial\omega}{\partial\eta}\right)_{\substack{\xi=0\\ \eta=B}}\right|_{max} = \sqrt{\frac{2}{\epsilon d}} \tag{5.33}$$

which occurs when

$$\eta = \sqrt{2\epsilon d} \tag{5.34}$$

Eq. (5.33) is valid only when the conditions given by Eq. (5.26) are satisfied.

Next, from Eqs. (5.16), (3.5), and (2.12):

$$\omega\frac{\partial\omega}{\partial\eta} \sim \frac{(W_o + c)}{\epsilon d c} \tag{5.35}$$

where, from Eqs. (5.22), (3.5), and (5.6):

$$w_0 = c\left(1 + \frac{2F}{AB}\right) \cong c, \quad \text{when } |F| << AB \tag{5.36}$$

Then, substituting Eq. (5.36) into (5.35) gives:

$$\omega \frac{\partial \omega}{\partial z} \sim \frac{2}{\epsilon d}, \quad \text{when } |F| << AB \tag{5.37}$$

Comparing Eqs. (5.37) and (5.33) when $\epsilon << 1$, it is apparent that the order of magnitude of "typical" inertia forces, given by Eq. (5.37), is much *greater* than the order of magnitude of the inertia forces given by Eq. (5.33) in the vicinity of the cross-section where the conditions of Eq. (5.26) are met.

The viscous forces are approximately zero when $AB \cong -F$ but they are *not* nearly zero for other values of AB; therefore, when $AB \cong -F$, both viscous and inertia forces are considerably smaller than they are elsewhere in the flow. To a first approximation, both viscous and inertia forces may be *neglected* when $AB \cong -F$; to this degree of approximation, Eq. (5.1) then becomes:

$$\frac{\partial p}{\partial z} \cong 0 \tag{5.38}$$

which says that there is no significant longitudinal pressure gradient when $AB \cong -F$. This indicates the existence there

of a stagnation point (or zone) in the lab frame, and a corresponding point (or zone) of uniform fluid velocity in the wave frame.

Eq. (5.38) is obtainable from the inertia-free theory alone at AB = - F [by using Eqs. (3.18), (3.15), (2.6), and (4.12)]; therefore, to a first approximation, the presence of the infinite Reynolds number singularity at AB = - F does not significantly affect the validity of the inertia-free theory results.

It is now necessary to find the maximum value of Re (apart from the large values of Re near the singularity). Say that the maximum value of Re on the centerline occurs when

$$\gamma = \gamma^{**} \tag{5.39}$$

Then assume that

$$|F| \ll (AB)\Big|_{\gamma^{**}} \tag{5.40}$$

This assumption will be verified a posteriori.

Then Eq. (5.31) becomes, near γ^{**}:

$$\left[\left(\frac{Re}{Rc/\nu}\right)_{\substack{\xi=0\\ \eta=B}}\right]_{\gamma\cong\gamma^{**}} \cong \left|\frac{\frac{dB}{d\gamma}\left[B\frac{dA}{dB}+A\right]\cdot F}{2\left[A^2+B^2\right]}\right|_{\gamma\cong\gamma^{**}} \tag{5.41}$$

Now for simplicity assume, when $\gamma \cong \gamma^{**}$, that the wall shape is given by:

$$B(\gamma) = \left[\frac{1}{4d}\gamma^2 + \frac{\epsilon}{2}\right] \tag{5.42}$$

and that Eq. (5.28) holds,

and make the following simplifying approximations:

$$\epsilon^2 << 1 \tag{5.43}$$

$$\left(\frac{\epsilon\gamma^2}{4d}\right) << 1 \text{ , when } \gamma \cong \gamma^{**} \tag{5.44}$$

$$\left(\frac{\gamma^2}{4d}\right)^4 << 1 \text{ , when } \gamma \cong \gamma^{**} \tag{5.45}$$

These three assumptions will also be verified a posteriori.

Then Eq. (5.41) becomes:

$$\left[\left(\frac{Re}{R\cdot c/\nu}\right)_{\substack{\xi=0\\ \eta=R}}\right]_{\gamma\cong\gamma^{**}} \cong \left|\frac{F}{4d}\frac{\left(\frac{\pi}{2}\gamma - \frac{3}{16}d^2\cdot\gamma^5\right)}{\left(\frac{\pi^2}{4} - \frac{(\pi-1)}{16\,d^2}\gamma^4\right)}\right|_{\gamma\cong\gamma^{**}} \tag{5.46}$$

Taking the derivative of Eq. (5.46) with respect to γ, equating the derivative to zero at $\gamma = \gamma^{**}$, and using Eq. (5.45), gives an approximate expression for γ^{**}:

$$\zeta^{**} \cong \left(\frac{8\pi^2}{9\pi+6}\right)^{1/4} d^{1/2} \cong (1.232)\, d^{1/2} \tag{5.47}$$

Substituting Eq. (5.47) into (5.46) then gives:

$$\left(\frac{Re}{R\cdot c/\nu}\right)_{\substack{\xi=0 \\ \eta=B \\ \zeta=\zeta^{**}}} \equiv \left(\frac{Re^{**}}{R\cdot c/\nu}\right) \cong -\alpha \cdot F \tag{5.48}$$

where

$$\alpha \equiv \frac{(0.161)}{d^{1/2}}\left[1-(0.675)\epsilon\right] \tag{5.49}$$

Eq. (5.48) is subject to the assumptions of Eqs. (5.17), (5.43), (5.40), (5.44), and (5.45). Eq. (5.47) is a consequence of these assumptions. Substituting Eq. (5.47) into Eqs. (5.40), (5.44),and (5.45) gives, respectively:

$$|F| << [(0.541)+(0.570)\epsilon] \tag{5.50}$$

$$(0.379)\epsilon << 1 \tag{5.51}$$

$$(0.0207) << 1 \tag{5.52}$$

Thus inequalities (5.40) and (5.43)-(5.45) are satisfied for $\epsilon < 10^{-1}$.

C. Conditions for Low Reynolds Number

Now it is possible to obtain the relations defining the

conditions under which the low Reynolds number condition is satisfied. Combining Eqs. (4.12), (3.24), and (3.28) gives:

$$F = \left[\frac{-\delta p_\lambda}{(\mu c/R)} \cdot \frac{1}{4F^\circ} - \frac{G^\circ}{F^\circ}\right] \tag{5.53}$$

Re** is the maximum Reynolds number on the centerline, except near the singularity. The inertia-free solution is expected to be valid if Re** $\leq$ 1. This condition then determines an upper bound for the flow rate which, on using Eqs. (5.48), (5.53), and (3.28), is written as (for Re** = 1):

$$\bar{Q}_{max} = \left[\frac{\pi R \nu\mu\left(\overline{AB} - \frac{G^\circ}{F^\circ}\right) - \frac{\alpha \cdot \pi R^3 \overline{AB} \cdot \delta p_\lambda}{4F^\circ}}{\alpha \cdot \left(\frac{G^\circ}{F^\circ}\right) \cdot \mu}\right] \tag{5.54}$$

For the modified Witch of Agnesi wave shape, $(1/4F^\circ)$ is given by Eq. (3.49), and the other coefficients are:

$$\left(\frac{G^\circ}{F^\circ}\right) \cong \frac{\pi\epsilon}{3} + O(\epsilon^3) \tag{5.55}$$

and

$$\overline{AB} \cong \left[1 - \frac{\sqrt{2md}}{L} \cdot \left(2 - \frac{\pi m}{6}\right)\right] \tag{5.56}$$

Substituting Eqs. (3.49), (5.55), and (5.56) into Eq. (5.54) gives (with m = 0.4 and $\epsilon << 1$):

$$\bar{Q}_{max} \cong \left\{(18.63)\left[1 - (1.60)\frac{d^{1/2}}{L}\right] \cdot \frac{R d^{1/2}}{\epsilon\mu} \cdot \left[\nu\mu - (0.00518)\frac{\delta p_\lambda R^2 \epsilon^{5/2}}{d}\right]\right\} \tag{5.57}$$

If the additional condition is imposed that the value of ϵ be such as to minimize I.H., i.e., that $\epsilon = \epsilon_o$, if Eq. (4.53) is assumed to be true (which will usually be a fairly good approximation) and if c is eliminated by using Eq. (4.54), then Eq. (5.57) becomes:

$$\bar{Q}_{max} \cong (2.267)\left[\frac{R^3 d^{1/6} \delta p_\lambda^{2/3} \cdot \nu}{\mu^{2/3}}\right]^{3/5} \tag{5.58}$$

For example, if the parameter values are chosen to be:

$$\begin{aligned} R &= 1.0 \text{ cm} \\ d &= 4. \\ \delta p_\lambda &= 1.5 \times 10^5 \text{ gm/cm sec}^2 \quad (=112.5 \text{ mm Hg}) \\ \nu &= 0.05 \text{ cm}^2/\text{sec} \\ \mu &= 0.05 \text{ gm/cm sec} \end{aligned} \tag{5.59}$$

then Eq. (5.58) gives:

$$\bar{Q}_{max} = 42.2 \text{ cm}^3/\text{sec} \tag{5.60}$$

$\bar{Q}_{max}$, as given by Eq. (5.58), is strongly dependent upon R ($\bar{Q}_{max} \sim R^{1.8}$), but is only weakly dependent upon δp_λ ($\bar{Q}_{max} \sim \delta p_\lambda^{0.4}$), and is practically independent of d ($\bar{Q}_{max} \sim d^{0.1}$).

5.2 Continuous Fluid

Eq. (3.1) is valid only if the fluid is continuous - i.e., only if the size of any solid particles in the fluid is small relative to the length scale of the macroscopic flow motion. Blood contains a variety of particle-like elements, the most

important of which are the red cells, which are typically shaped as biconcave discs with a mean diameter of about 8 microns and a maximum thickness of about 2 microns.[19] In order for Eq. (3.1) to be applicable to flow of blood through a peristaltic pump, it is necessary to require that the smallest natural length scale of the pump be much greater than 8 microns. That is, require:

$$\epsilon \cdot R \gg 8 \text{ microns} = 8 \times 10^{-4} \text{cm} \tag{5.61}$$

For example, if R = 1 cm, then Eq. (5.61) requires:

$$\epsilon \gg 8 \times 10^{-4} \sim 10^{-3} \tag{5.62}$$

Eq. (5.61) is particularly applicable to Eqs. (4.47) and (5.58).

6. SUMMARY AND CONCLUSIONS

In this paper, an extensive mathematical model of peristaltic-type (primarily roller-type) blood pumps has been developed. Analytic and numerical results were obtained by making certain simplifying geometric and boundary condition approximations and by making certain additional dynamical and physical approximations (e.g., inertia-free flow; negligible longitudinal gradients of longitudinal fluid velocity; and Newtonian fluid.).

Significant results include:

(i) The determination of the analytic linear relationship between pressure rise per wave length and volume flow rate (δp_λ vs. $\bar{Q}$) in pumping; see Eqs. (3.28), (3.37), and (3.47).

(ii) The development of a criterion giving the form of the analytic relationship between the Index of Hemolysis (I.H.) and the dynamic and geometric pump parameters.

(iii) This criterion was applied to the cases of pumps having the square and modified Witch of Agnesi wave shape geometries; see Eqs. (4.9), (4.37), and (4.46) .

(iv) Determination of an optimum setting of the degree of occlusion to minimize the Index of Hemolysis (as given by the hemolysis criterion) for the Witch of Agnesi wave shape; see Eqs. (4.47) and (4.55).

(v) Determination of the range of validity of the theory under the inertia-free flow and continuous fluid hypotheses.

The potential value of this work lies in its reduction

of qualitatively well-understood phenomena (e.g., pressure rise vs. flow during pumping) to analytic form, and in its extension of analytic investigation to phenomena which were previously unexplained or only poorly understood (e.g., the phenomenon of hemolysis in roller pumps, and the phenomenon of an optimum degree of occlusion for minimizing the hemolysis index.)

APPENDIX 1

Derivation of the Value of I.H. for the Normal Heart and Circulatory System

[See Section 1.3]

The average lifespan of a red blood cell is 120 days under normal *in vivo* conditions (Ref. 19, pp. 118-119). Whole blood contains an average of 15 grams of hemoglobin per 100 ml (Ref. 19, p. 111). The average blood volume of a normal adult is about 5000 ml (Ref. 19, p. 419). Average cardiac output is about 5000 ml/min (Ref. 19, p. 265). 5000 ml of blood is hemolyzed in 120 days. Therefore:

$$\text{I.H.} = \left(\frac{15 \times 10^3 \text{ mg Hb}}{100 \text{ ml. blood}}\right) \times \left(\frac{5000 \text{ ml. blood}}{120 \text{ days}}\right) \times \left(\frac{1 \text{ day}}{1440 \text{ min}}\right) \times$$

$$\times \left(\frac{1 \text{ min}}{5000 \text{ ml. pumped}}\right) = 0.0868 \left(\frac{\text{mg. Hb released}}{100 \text{ ml. blood pumped}}\right)$$

Q.E.D.

APPENDIX 2

Derivation of Eq. (2.9)

Writing Eq. (2.4) in dimensionless form (using Eq. (2.6) and the definition of $R \equiv P/2\pi$) gives:

$$2\pi = 4A \cdot \int_0^{\pi/2} \left[1 - \left(\frac{A^2-B^2}{A^2}\right) \sin^2 w\right]^{1/2} dw \equiv 4A \cdot E\left(\frac{A^2-B^2}{A^2}\right) \quad \text{(A 2.1)}$$

Now a numerical procedure is developed for computing A as a function of B.

$$\text{Define:} \quad D \equiv \left(\frac{A^2-B^2}{A^2}\right) \quad \text{(A 2.2)}$$

Then, by Eq. (A 2.1),

$$A = \frac{\pi}{2E(D)} \qquad \text{(A 2.3)}$$

And, by Eq. (A 2.2),

$$B = (1-D)^{1/2} \cdot A(D) \qquad \text{(A 2.4)}$$

Very accurate numerical formulas for E(D) exist (e.g., see Ref. 20). Table 1 was constructed by choosing different values of D and then using Eqs. (A 2.3) and (A 2.4) to get corresponding values of A and B.

For small values of B, A is expressible as a Maclaurin series in B:

$$A \cong A(0) + \left.\frac{dA}{dB}\right|_{B=0} \cdot B + \left.\frac{d^2A}{dB^2}\right|_{B=0} \cdot \frac{B^2}{2!} + \cdots \qquad \text{(A 2.5)}$$

It is easy to show, by differentiating Eq. (A 2.1) with respect to A, that

$$\left.\frac{dA}{dB}\right|_{B=0} = 0 \qquad \text{(A 2.6)}$$

and it is evident that

$$A(0) = \frac{\pi}{2} \qquad \text{(A 2.7)}$$

[The author was unable to analytically evaluate $\left.\frac{d^2A}{dB^2}\right|_{B=0}$.]

Therefore, defining

$$\frac{1}{2!}\frac{d^2A}{dB^2} \equiv -\alpha \qquad \text{(A 2.8)}$$

Eq. (A 2.5) becomes:

$$A \cong \frac{\pi}{2} - \alpha \cdot B^2 + O(B^3) \qquad \text{(A 2.9)}$$

For small B, Eq. (A 2.9) gives:

$$\alpha \cong \left(\frac{\frac{\pi}{2} - A}{B^2}\right) \qquad \text{(A 2.10)}$$

Values of α, as computed by Eq. (A 2.10) - using the tabulated values of A and B (which are accurate only to 5 or 6 significant digits) - are listed in Table 1. Taking into account roundoff error and the effect of B getting large, it is easily seen that a reasonable range, in which the actual value of the constant α should lie, is:

$$0.7 \leq \alpha \leq 1.7 \qquad \text{(A 2.11)}$$

This establishes Eq. (2.9).

Q.E.D.

APPENDIX 3

Derivation of Eq. (4.11)

For simplicity, it will be *assumed* that $\underset{\sim}{n}$, the unit inner normal vector to the wall, has no z-component, so that:

$$\underset{\sim}{n} = (n_x , n_y) \tag{A 3.1}$$

Neglecting the z-component of ∇w gives:

$$\nabla w = \left(\frac{\partial w}{\partial x} , \frac{\partial w}{\partial y} \right) \tag{A 3.2}$$

[The preceding two assumptions, and the assumption that shear forces due to transverse components of velocity are negligible, will be approximately correct whenever $\frac{dB}{dz}$ is sufficiently small everywhere along the tube.]

From Eqs. (2.3) and (2.11), the equation of the tube wall is:

$$J(x,y) = \left[\frac{x^2}{a^2} + \frac{(y-b)^2}{b^2} - 1 \right] = 0 \tag{A 3.3}$$

where the z-dependence of "a" and "b" is neglected. Then:

$$(n_x , n_y) = \frac{-\nabla J}{\|\nabla J\|} = \frac{-\left[\frac{x}{a^2} , \frac{y-b}{b^2} \right]}{\left[\left(\frac{x}{a^2} \right)^2 + \left(\frac{y-b}{b^2} \right)^2 \right]^{1/2}} \tag{A 3.4}$$

From Eqs. (3.5), (3.6), (2.12), and (2.6), the longitudinal velocity is:

$$w = \left\{ -c - \frac{R}{2\mu} \frac{dp}{d\gamma} \frac{a^2 b^2}{(a^2+b^2)} \left[1 - \frac{x^2}{a^2} - \frac{(y-b)^2}{b^2} \right] \right\} \qquad \text{(A 3.5)}$$

so that Eq. (A 3.2) becomes:

$$\nabla w = \frac{a^2 b^2}{(a^2+b^2)} \cdot \frac{1}{R\mu} \cdot \frac{dp}{d\gamma} \cdot \left[\frac{x}{a^2} , \frac{y-b}{b^2} \right] \qquad \text{(A 3.6)}$$

Substituting Eqs. (A 3.6) and (A 3.4) into Eq. (4.10), and using Eqs. (2.12) and (2.6) gives:

$$\tau_{wall} = \frac{A^2 B^2}{A^2+B^2} \cdot \frac{dp}{d\gamma} \cdot \left[\frac{\xi^2}{A^4} + \frac{(\eta-B)^2}{B^4} \right]^{1/2} \qquad \text{(A 3.7)}$$

on the wall at (ξ, η). But on the wall, the relation

$$\frac{\xi^2}{A^2} + \frac{(\eta-B)^2}{B^2} = 1 \qquad \text{(A 3.8)}$$

holds. Also, from Eq. (3.17):

$$\left(\frac{A^2 B^2}{A^2+B^2} \cdot \frac{dp}{d\gamma} \right) = -\frac{4\mu c}{R} \left[\frac{q}{\pi AB R^2 c} + 1 \right] \qquad \text{(A 3.9)}$$

So, substituting Eqs. (A 3.8), (A 3.9), and (4.12) into (A 3.7), gives Eq. (4.11) as the desired approximate expression for the shear stress distribution on the wall.

Q.E.D.

APPENDIX 4

Derivation of Eq. (4.46)

It is first necessary to determine the sign of the

quantity r, defined by Eq. (4.43). r = 0 when

$$\gamma = \gamma_0 \equiv \sqrt{2d\left(-\frac{4}{\pi}F - \epsilon\right)} \qquad \text{(A 4.1)}$$

It follows from Eq. (4.43) that

$$r(\gamma = 0) \leq 0 \qquad \text{(A 4.2)}$$

if and only if

$$(-F) \geq \frac{\pi\epsilon}{4} \qquad \text{(A 4.3)}$$

Using Eqs. (5.53) and (5.55), it is easy to see that Eq. (A 4.3) is satisfied whenever Eqs. (4.40)and (4.41) are true; therefore Eq. (A 4.2) is true. It then follows that:

$$\int_0^{\sqrt{2md}} |r|\, d\gamma = \left[-2\cdot\int_0^{\gamma_0} r\, d\gamma + \int_0^{\sqrt{2md}} r\, d\gamma\right] \qquad \text{(A 4.4)}$$

Finally then, Eq. (4.44), with substitutions from Eqs. (A 4.4), (A 4.1), (4.38), (4.39), (5.53), and (4.45), becomes Eq. (4.46),as desired.

Q.E.D.

APPENDIX 5

Derivation of Eq. (4.47)

The objective is to find the value of ϵ at which I.H., as given by Eq. (4.46), has its minimum value. Define:

$$u \equiv \left(\frac{\delta p_\lambda \cdot R}{\mu c}\right) \cdot \left(\frac{\epsilon^{3/2}}{\pi 2^{3/2} d^{1/2}}\right) \tag{A 5.1}$$

from which it follows that:

$$\left(\frac{\delta p_\lambda \cdot R}{\mu c}\right) \epsilon = \frac{\pi 2^{3/2} d^{1/2}}{\epsilon^{1/2}} \cdot u \tag{A 5.2}$$

and

$$\left(\frac{\mu c}{\delta p_\lambda \cdot R}\right) \cdot \frac{d}{\epsilon^2} = \frac{d^{1/2}}{u \epsilon^{1/2} \pi 2^{3/2}} \tag{A 5.3}$$

Substituting Eqs. (A 5.1), (A 5.2), and (A 5.3) into Eq. (4.46), yields:

$$\begin{aligned} \text{I.H.} = f(\epsilon, u) \equiv \Bigg[& \frac{16 \pi k^* \mu c R}{\bar{Q}} \cdot \frac{d^{1/2}}{\epsilon^{1/2}} \cdot \\ & \cdot \Bigg\{ \frac{\pi^2}{3 \cdot 2^{3/2}} [2-u] \cdot \left[\frac{1}{2} - \frac{2}{\pi} \tan^{-1}\left(\frac{1}{3^{1/2}} [1+u]^{1/2}\right)\right] \\ & + \frac{\pi}{2^{1/2} 3^{1/2}} [1+u]^{1/2} \Bigg\} + \frac{16 \pi k^* \mu c R}{\bar{Q}} \cdot \\ & \cdot \left\{ \frac{-\pi d^{1/2}}{2^{1/2} m^{1/2}} + \frac{L}{2} - 2^{1/2} m^{1/2} d^{1/2} \right\} \Bigg] \end{aligned} \tag{A 5.4}$$

Differentiating Eq. (A 5.4) with respect to ϵ by the chain rule gives:

$$\frac{\partial \text{I.H}}{\partial \epsilon} = \left[\frac{\partial f(\epsilon, u)}{\partial \epsilon} + \frac{\partial f(\epsilon, u)}{\partial u} \cdot \frac{\partial u}{\partial \epsilon} \right] \tag{A 5.5}$$

where, by Eq. (A 5.1)

$$\frac{\partial u}{\partial \epsilon} = \frac{\delta p_\lambda \cdot R}{\mu c} \cdot \frac{3 \epsilon^{1/2}}{\pi 2^{5/2} d^{1/2}} = \frac{3u}{2\epsilon} \tag{A 5.6}$$

Substituting Eqs. (A 5.4) and (A 5.6) into Eq. (A 5.5) yields:

$$\frac{\partial I.H.}{\partial \epsilon} = \left[-\frac{2^{9/2}\pi^2}{3^{1/2}} \cdot \frac{k^* \mu c R}{\bar{Q}} \cdot \frac{d^{1/2}}{\epsilon^{3/2}} \cdot \frac{(u+1)^{1/2}}{(u+4)} \right] \cdot G(u) \qquad \text{(A 5.7)}$$

where

$$G(u) \equiv \left\{ \frac{\pi}{4 \cdot 3^{1/2}} (u+4)(u+1)^{1/2} \cdot \right.$$

$$\left. \cdot \left[\frac{1}{2} - \frac{2}{\pi} \tan^{-1}\left(\frac{1}{3^{1/2}} \cdot [1+u]^{1/2} \right) \right] - \frac{1}{2}(u-2) \right\} \qquad \text{(A 5.8)}$$

By inspection, a root of G(u) is

$$u = u_0 = 2 \qquad \text{(A 5.9)}$$

Substituting Eq. (A 5.9) into (A 5.1) yields Eq. (4.47) as the value of ϵ which makes $\partial(I.H)/\partial\epsilon$ equal to zero.

Figure 19 confirms that the extremum of I.H. at $\epsilon = \epsilon_o$ is indeed a *minimum* (and not a maximum).

Q.E.D.

TABLE 1

Computed Values of A = A(B)

B	$A_{accurate}$	A_{approx}	α
0.00000×10^{0}	1.57079	1.60000	(-5.01×10^{-6})
1.11131×10^{-2}	1.57056	1.59771	+1.80
1.92360 "	1.57017	1.59596	1.66
2.93669 "	1.56946	1.59370	1.53
3.99902 "	1.56848	1.59121	1.44
4.95671 "	1.56741	1.58888	1.37
6.06495 "	1.56595	1.58608	1.31
6.99715 "	1.56457	1.58363	1.27
7.81628 "	1.56323	1.58142	1.24
9.23326 "	1.56068	1.57744	1.19
9.86291 "	1.55945	1.57562	1.17
1.10102×10^{-1}	1.55706	1.57221	1.13
1.20431 "	1.55475	1.56904	1.11
1.29893 "	1.55251	1.56606	1.08
1.38666 "	1.55033	1.56322	1.06
1.50798 "	1.54716	1.55920	1.04
1.88157 "	1.53629	1.54603	0.97
2.99061 "	1.49530	1.50042	0.84
4.08369 "	1.44380	1.44639	0.76
5.32051 "	1.37375	1.37482	0.70
5.96070 "	1.33285	1.33347	0.67
6.92908 "	1.26507	1.26526	0.64
7.95269 "	1.18551	1.18550	0.61
9.09262 "	1.08677	1.08678	0.59
9.99999 "	9.99999×10^{-1}	1.00000	0.57

B and $A_{accurate}$ computed by method of Appendix 2.

A_{approx} computed from B by use of Eq. (2.8).

α computed by using B and $A_{accurate}$ in Eq. (A 2.10).

TABLE 2

Computed Values of Pressure-Flow Coefficients

h	d	ϵ	γ^*	L	1/4F°	G°/F°	$\overline{AB}$	$1/4F°_m$	$G°/F°_m$	$\overline{AB}_m$
2.0	8.0	.0001	8.0	20.	1.04E-12	1.06E-4	.6323	1.04E-12	1.05E-4	.7735
2.0	8.0	.001	8.0	20.	3.28E-10	1.06E-3	.6327	3.29E-10	1.05E-3	.7735
2.0	8.0	.01	8.0	20.	1.04E-7	1.05E-2	.6359	1.04E-7	1.05E-2	.7735
2.0	8.0	.1	8.0	20.	3.22E-5	1.08E-1	.6683	3.29E-5	1.05E-1	.7735
2.0	1.0	.0001	8.0	20.	2.94E-12	1.06E-4	.8376	2.95E-12	1.05E-4	.9199
2.0	1.0	.001	8.0	20.	9.29E-10	1.06E-3	.8377	9.32E-10	1.05E-3	.9199
2.0	1.0	.01	8.0	20.	2.94E-7	1.06E-2	.8392	2.95E-7	1.05E-2	.9199
2.0	1.0	.1	8.0	20.	8.86E-5	1.18E-1	.8545	9.32E-5	1.05E-1	.9199
2.0	8.0	.0001	8.0	80.	1.04E-12	1.06E-4	.9081	1.04E-12	1.05E-4	.9434
2.0	8.0	.001	8.0	80.	3.28E-10	1.06E-3	.9082	3.29E-10	1.05E-3	.9434
2.0	8.0	.01	8.0	80.	1.04E-7	1.06E-2	.9090	1.04E-7	1.05E-2	.9434
2.0	8.0	.1	8.0	80.	3.17E-5	1.21E-1	.9171	3.29E-5	1.05E-1	.9434
2.0	1.0	.0001	8.0	80.	2.94E-12	1.06E-4	.9594	2.95E-12	1.05E-4	.9800
2.0	1.0	.001	8.0	80.	9.29E-10	1.06E-3	.9594	9.32E-10	1.05E-3	.9800
2.0	1.0	.01	8.0	80.	2.93E-7	1.07E-2	.9598	2.95E-7	1.05E-2	.9800
2.0	1.0	.1	8.0	80.	8.50E-5	1.54E-1	.9636	9.32E-5	1.05E-1	.9800
1.0	8.0	.0001	8.0	20.	1.04E-12	1.06E-4	.4479	1.04E-12	1.05E-4	.7735
1.0	8.0	.001	8.0	20.	3.28E-10	1.06E-3	.4483	3.29E-10	1.05E-3	.7735
1.0	8.0	.01	8.0	20.	1.04E-7	1.06E-2	.4514	1.04E-7	1.05E-2	.7735
1.0	8.0	.1	8.0	20.	3.10E-5	1.13E-1	.4828	3.29E-5	1.05E-1	.7735
1.0	1.0	.0001	8.0	20.	2.94E-12	1.06E-4	.5810	2.95E-12	1.05E-4	.9199
1.0	1.0	.001	8.0	20.	9.29E-10	1.06E-3	.5811	9.32E-10	1.05E-3	.9199
1.0	1.0	.01	8.0	20.	2.93E-7	1.07E-2	.5827	2.95E-7	1.05E-2	.9199
1.0	1.0	.1	8.0	20.	8.32E-5	1.32E-1	.5982	9.32E-5	1.05E-1	.9199

Subscript "m" on column heading denotes "modified Witch of Agnesi" formulae used to compute numerical values. Columns without "m"'s were computed by numerical integration. Accuracy of numerical integration: ± 2 in least significant decimal place of all above.

$$A = A(B)$$

[Based on Table 1]

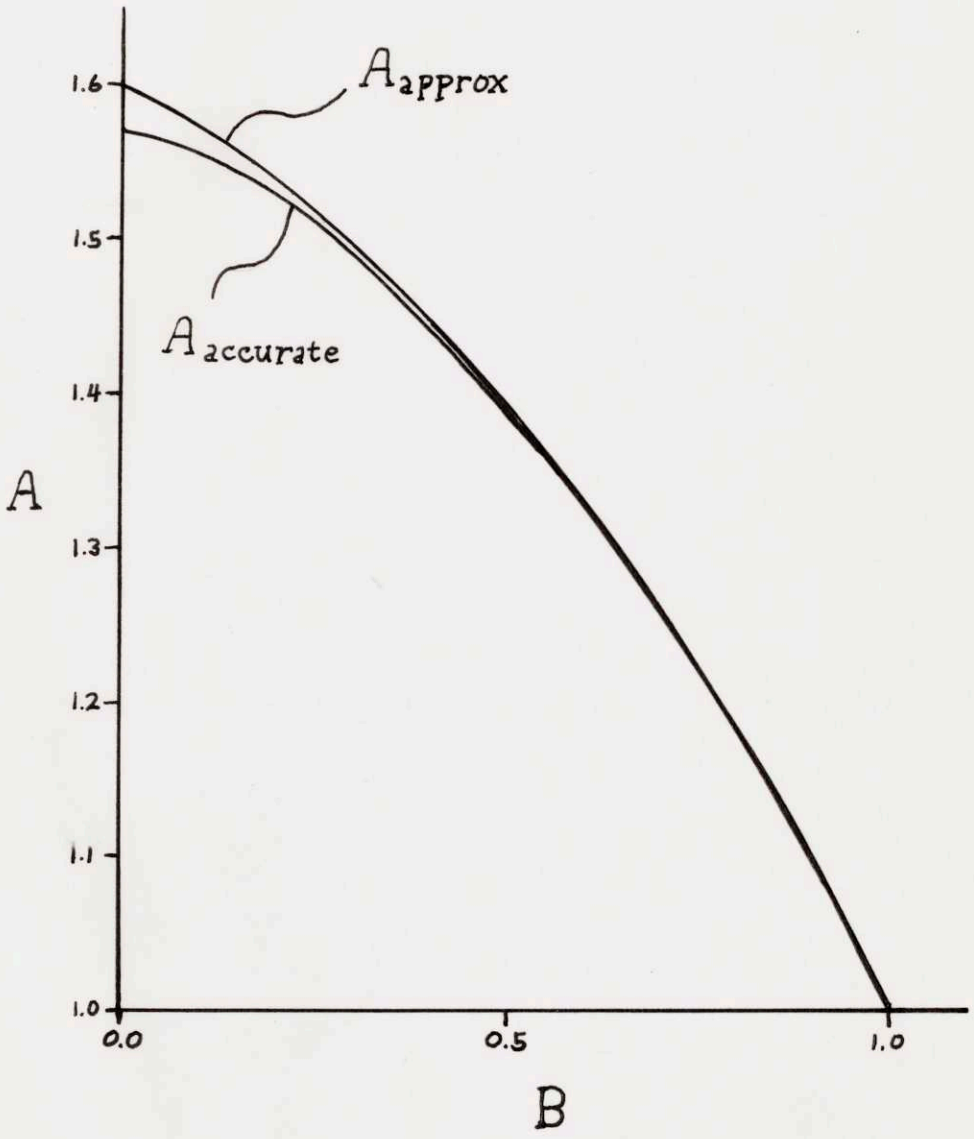

Figure 1

Figure 2

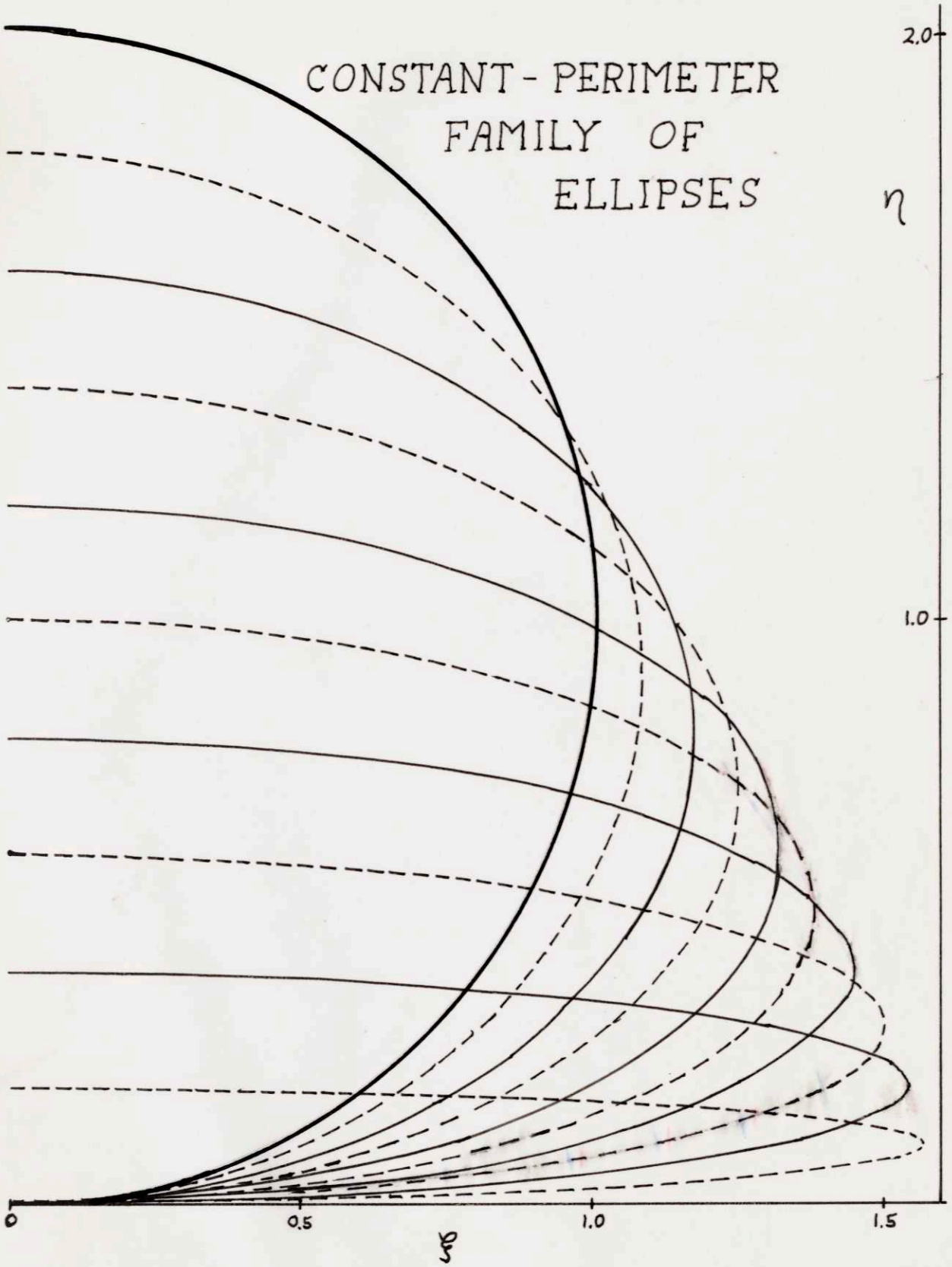

Figure 3

TYPICAL WAVE SHAPE OF ROLLER PUMP

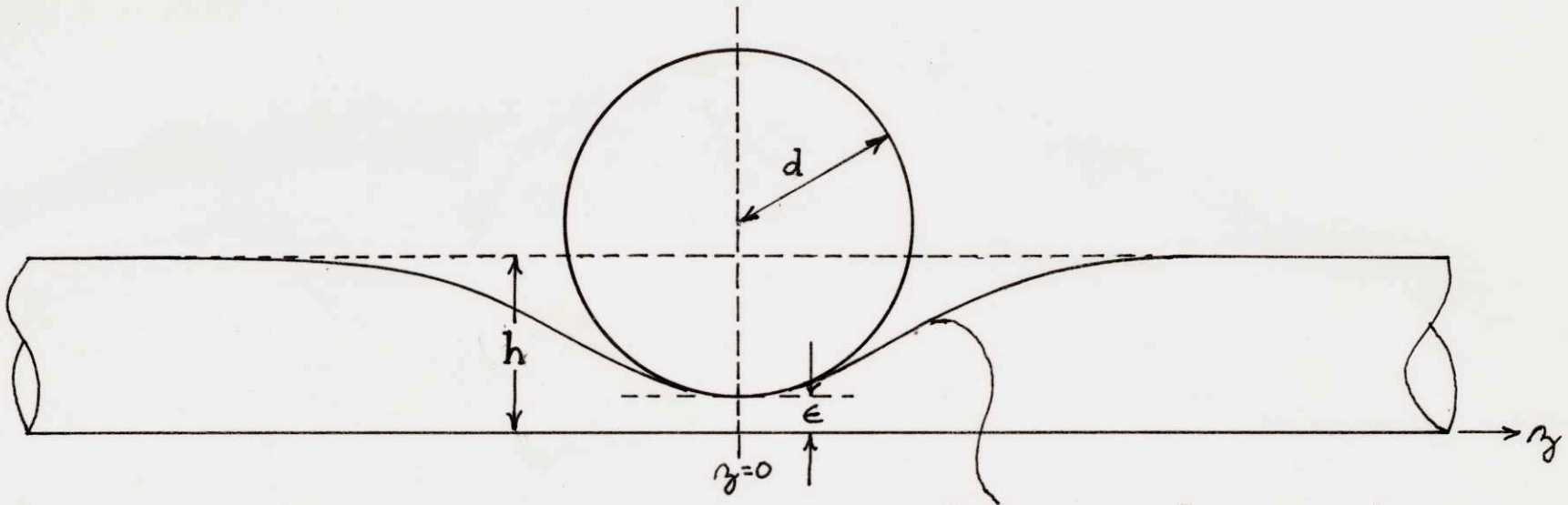

R = Inside Radius of undeformed tube.

All lengths are made dimensionless by dividing by R.

Longitudinal-vertical cross-section of inner wall of tube.

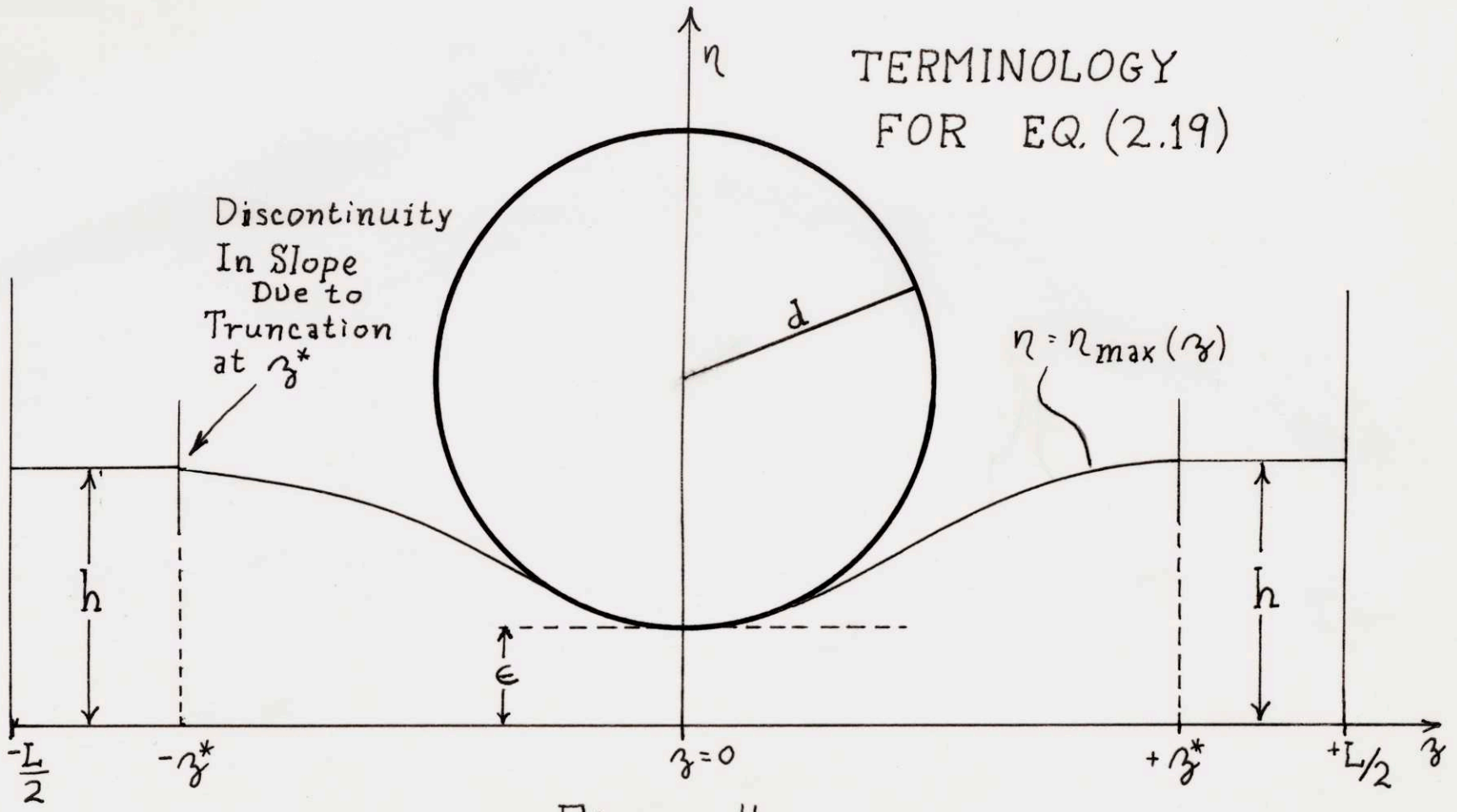
TERMINOLOGY
FOR EQ. (2.19)
η
Discontinuity
In Slope
Due to
Truncation
at ζ*
d
η = η_max(ζ)
h
h
ε
-L/2
-ζ*
ζ=0
+ζ*
+L/2
ζ

Figure 4

Figure 5

A Comparison of Eqs. (2.19) and (2.20)

The Case:

$d = 5.0$

$\epsilon = 0.0$

$h = 2.0$

$\gamma^* = 8.0$

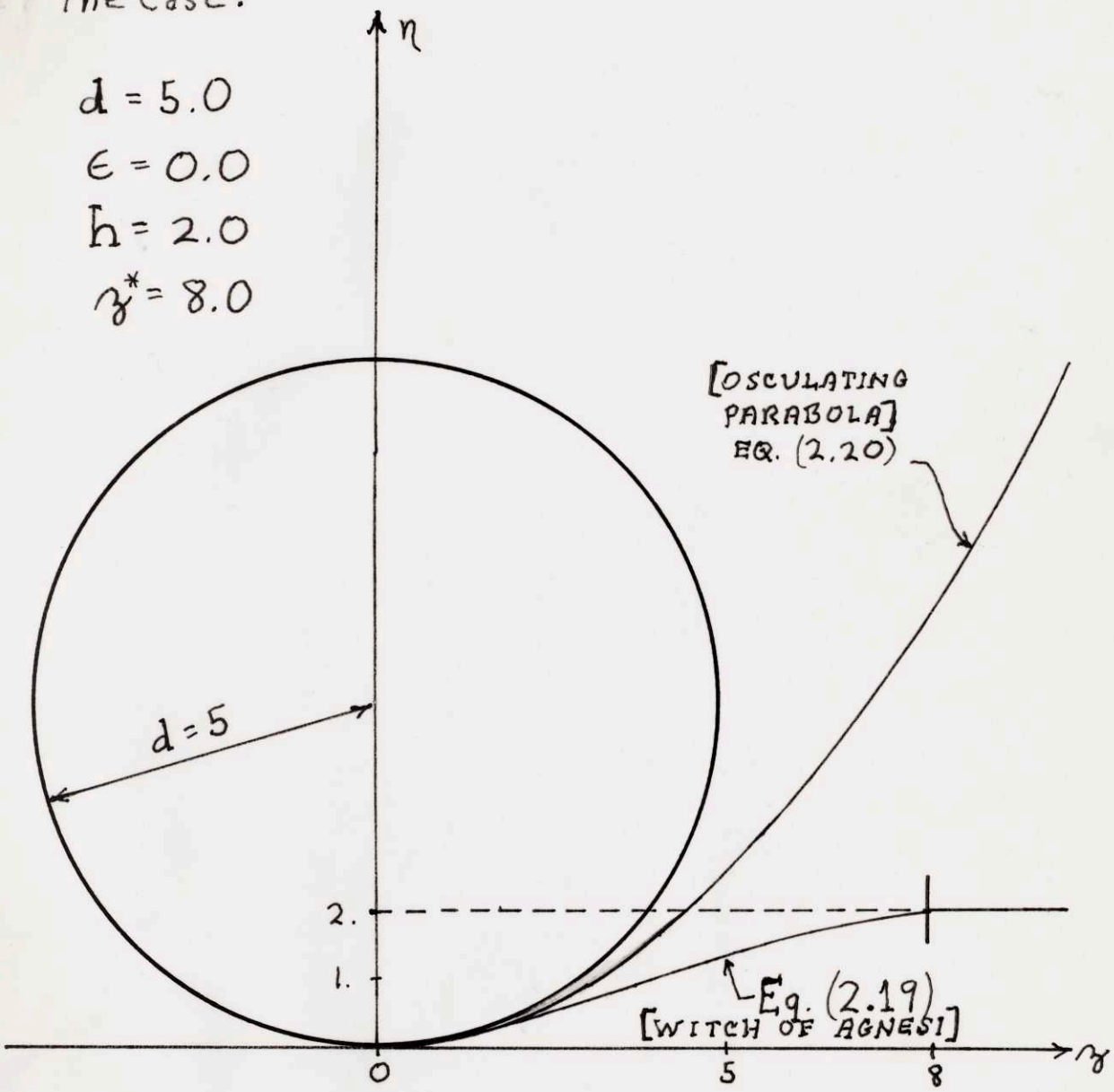

Tube No. 1

Wall Thickness = 3/16 in.

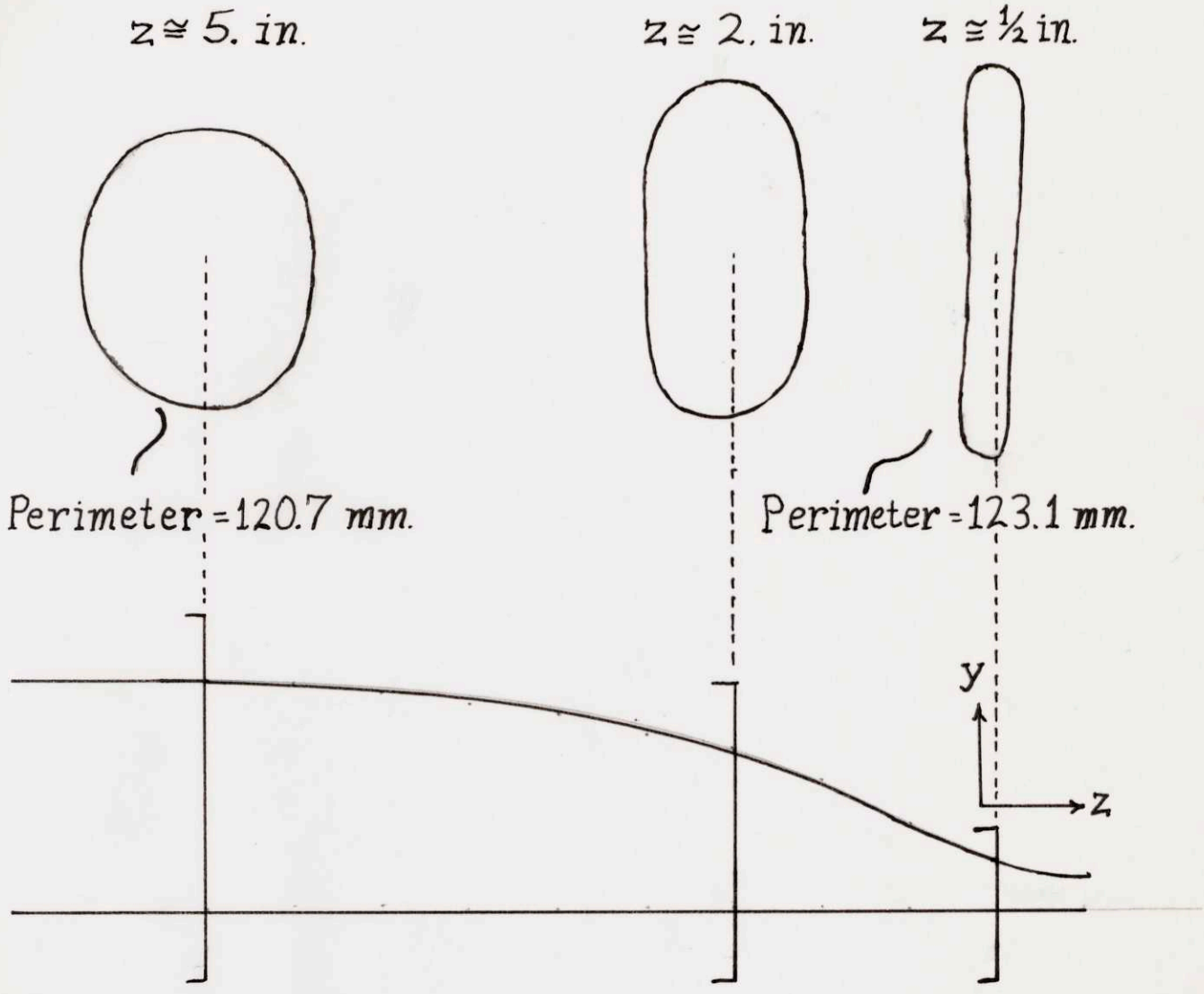

Longitudinal - Vertical Tube Profile

Figure 6

CONSTANT-PERIMETER TEST

Tube No. 2

Wall Thickness = 1/4 in.

z ≅ 2. in.

Perimeter = 31.2 mm.

z ≅ 1/4 in.

Perimeter = 31.1 mm.

Figure 7

CONSTANT-PERIMETER TEST

ANALYTIC FIT TO EMPIRICAL WAVE SHAPE

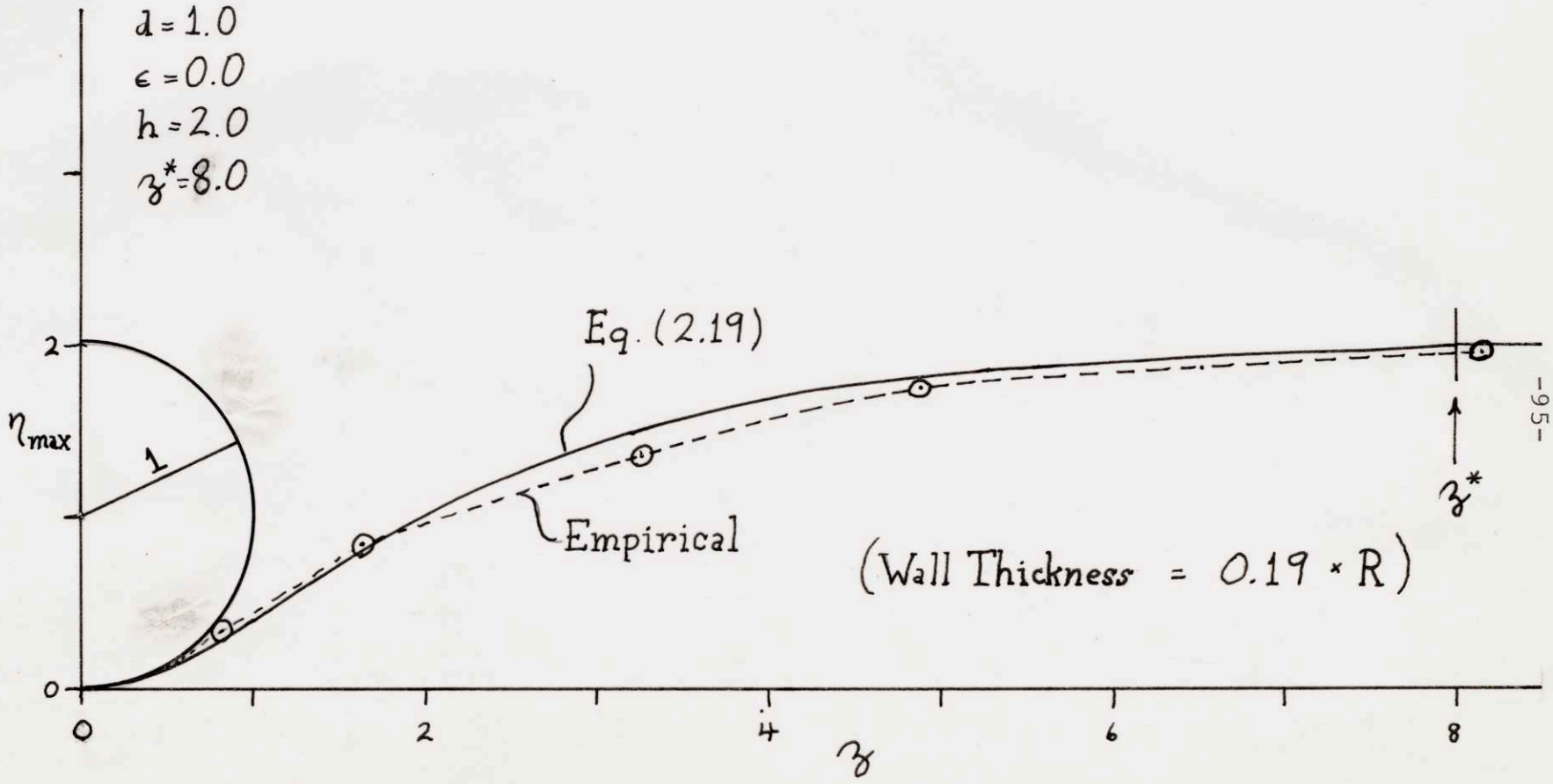

Figure 8

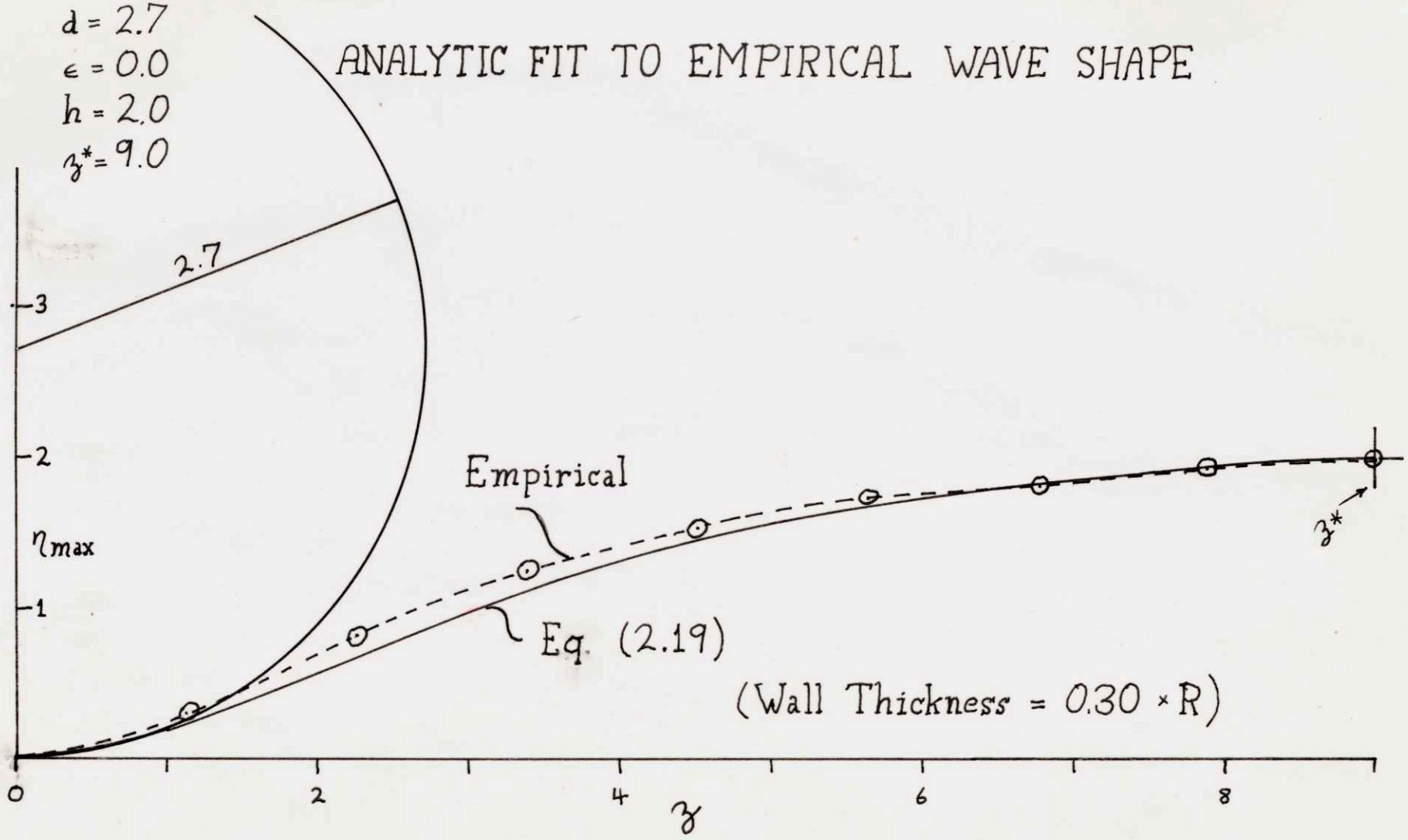
ANALYTIC FIT TO EMPIRICAL WAVE SHAPE
d = 2.7
ϵ = 0.0
h = 2.0
z* = 9.0
2.7
3
2
1
ηmax
Empirical
Eq. (2.19)
(Wall Thickness = 0.30 × R)
z*
0
2
4
6
8
z

Figure 9

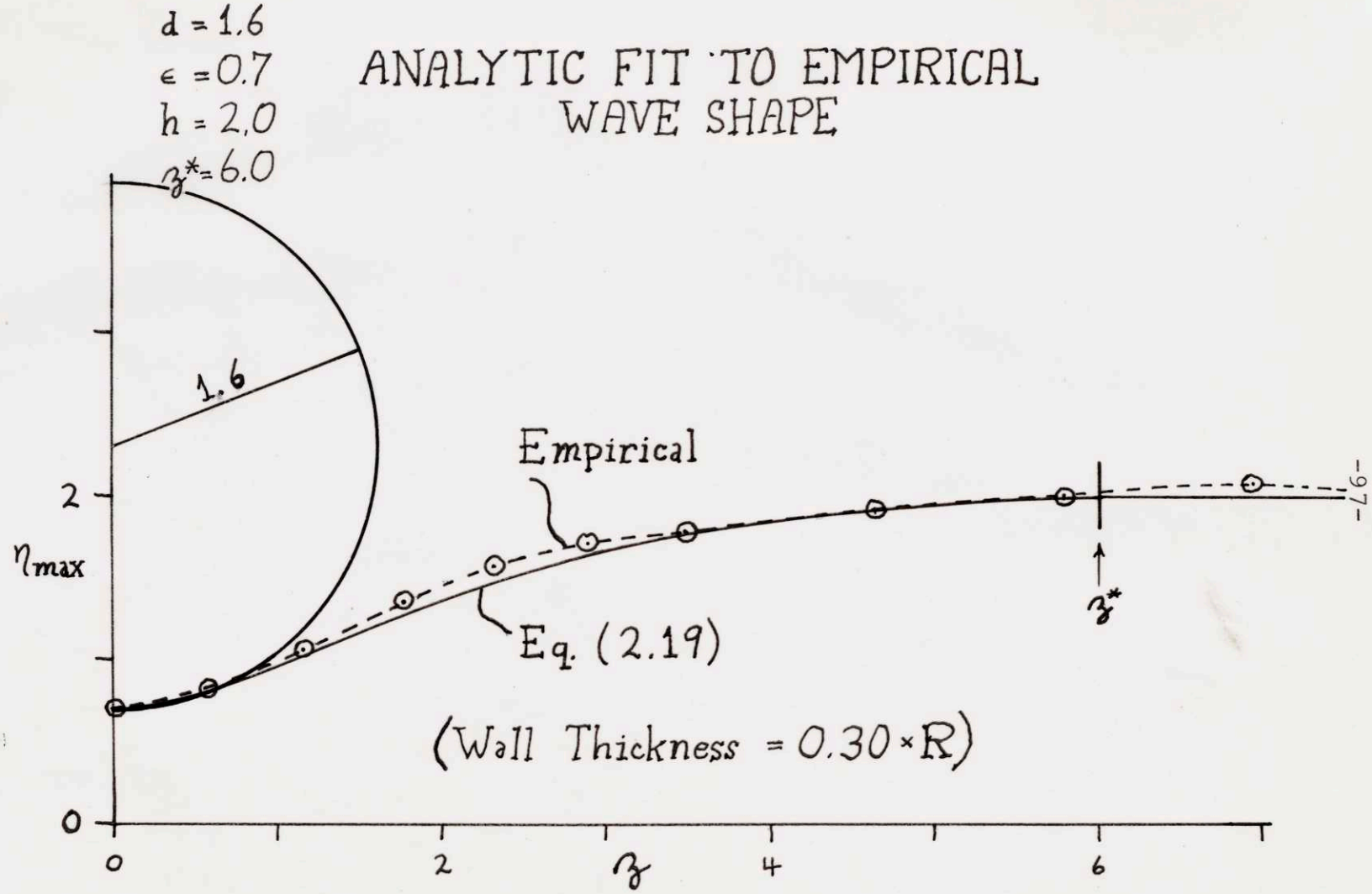
d = 1.6
ϵ = 0.7
h = 2.0
z* = 6.0
ANALYTIC FIT TO EMPIRICAL
WAVE SHAPE
1.6
Empirical
Eq. (2.19)
(Wall Thickness = 0.30 × R)
η max
z*
z
0
2
4
6
0
2

Figure 10

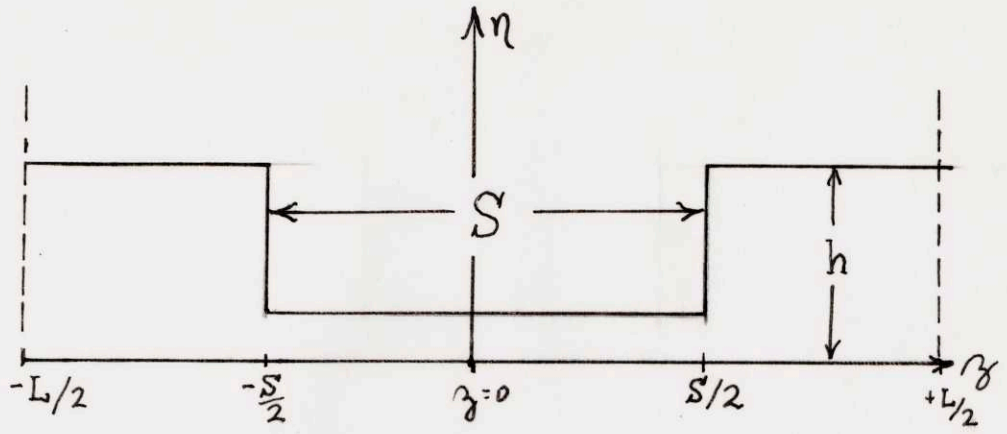

Figure 11 : SQUARE WAVE

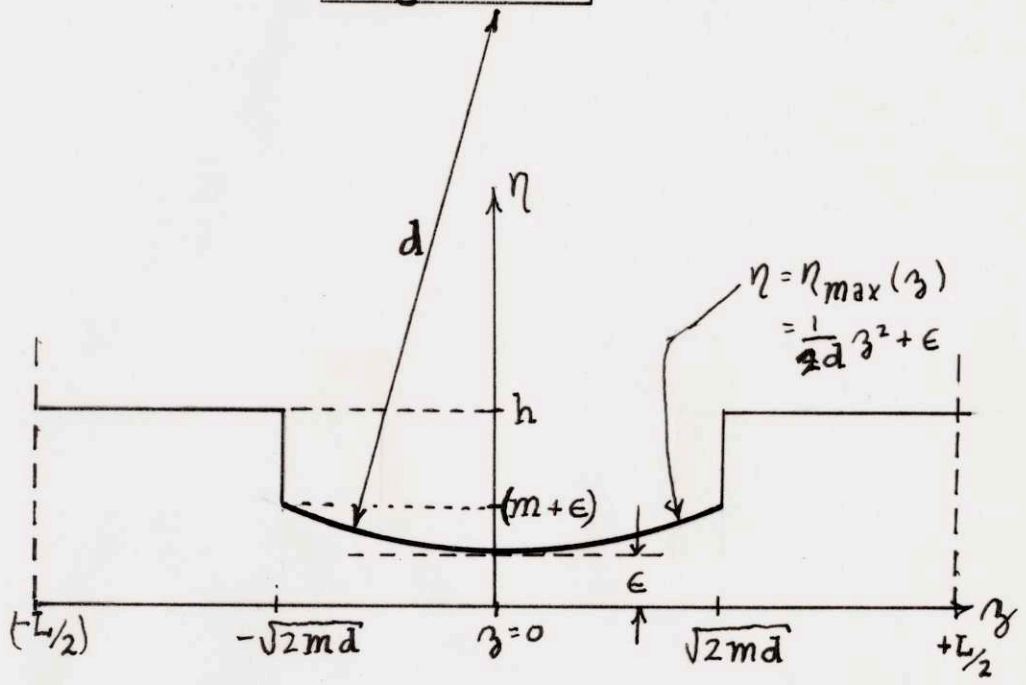

Figure 13
MODIFIED WITCH OF AGNESI WAVE

APPROXIMATE SQUARE WAVE

BASIC IDEA: USE SEVERAL SMALL ROLLERS CLOSE TOGETHER TO OBTAIN AN APPROXIMATELY UNIFORM DEGREE OF COMPRESSION ALONG A FINITE LENGTH OF THE TUBE.

[CREDIT: THE BASIC IDEA WAS ASCHER H. SHAPIRO's; SEE NOTE ON PAGE 37.]

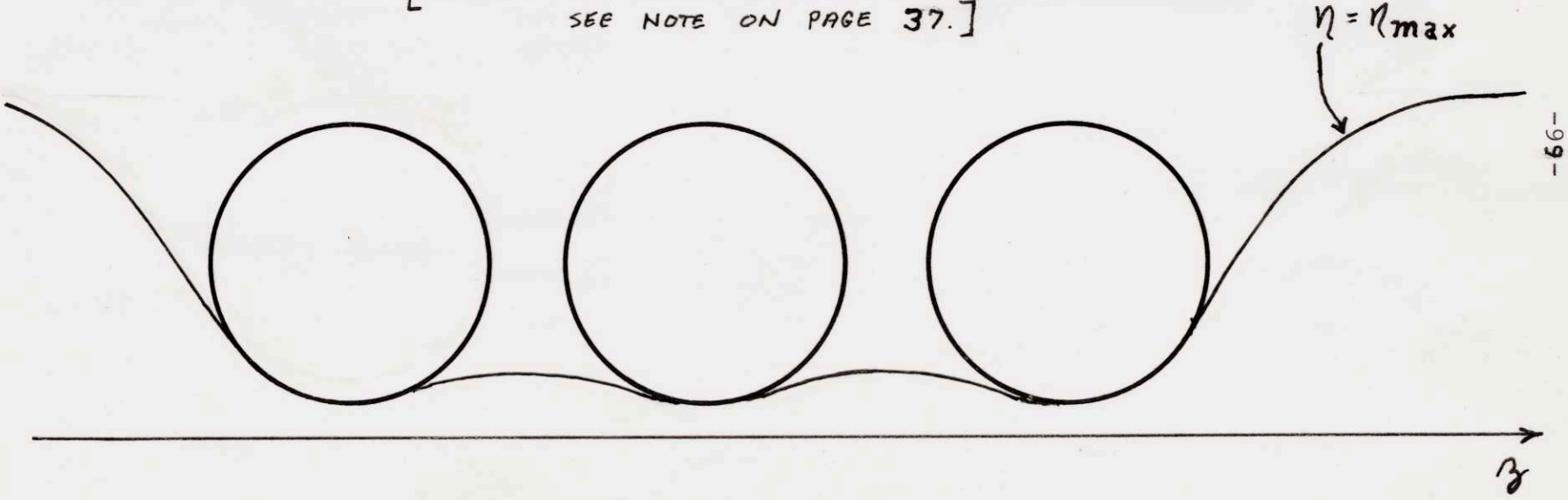

Figure 12

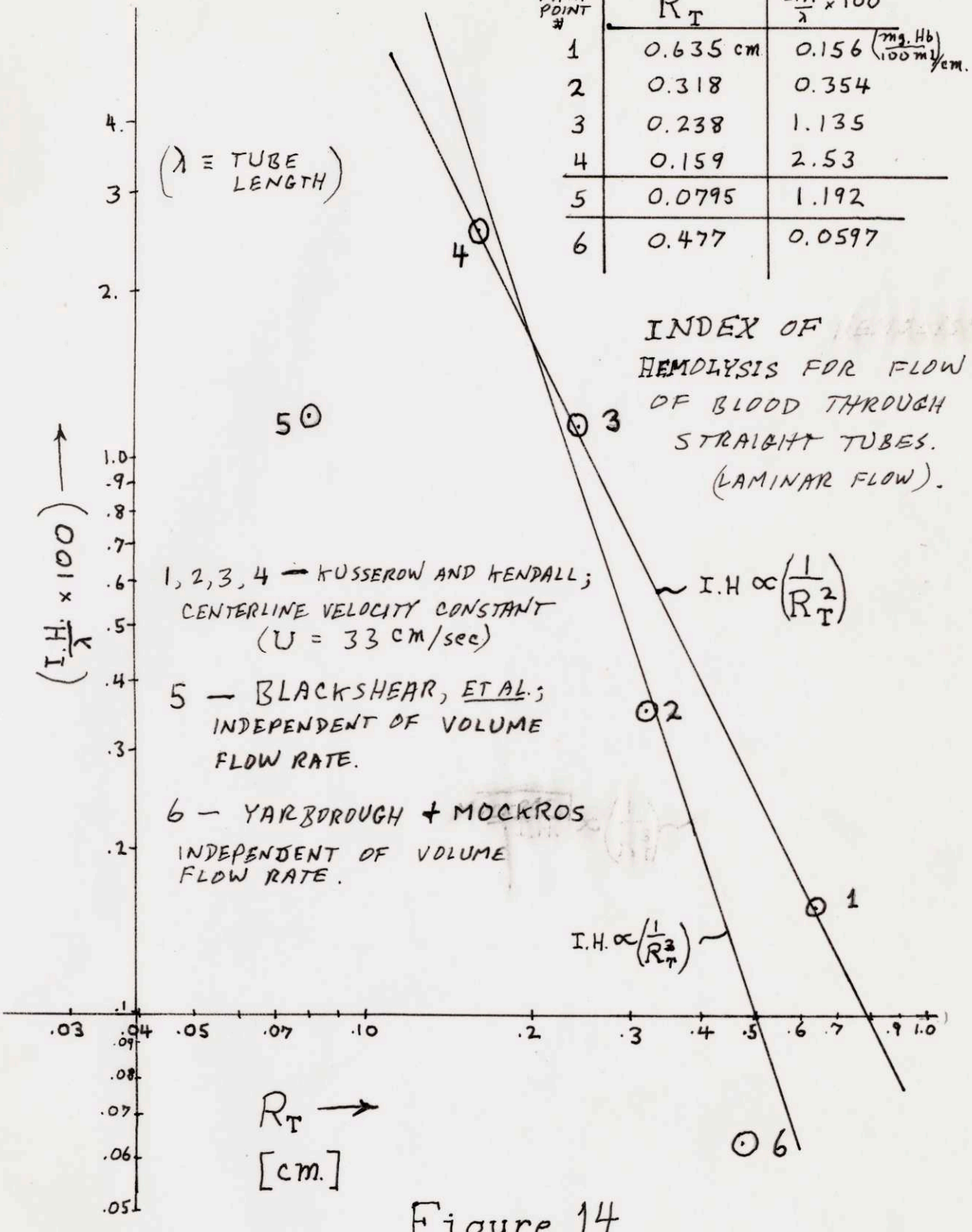

DATA POINT #	R_T	$\frac{I.H}{\lambda} \times 100$
1	0.635 cm	0.156 $\left(\frac{mg.Hb}{100\,ml}\right)/cm.$
2	0.318	0.354
3	0.238	1.135
4	0.159	2.53
5	0.0795	1.192
6	0.477	0.0597

Figure 14

DATA ON HEMOLYSIS (DATA FROM REFERENCE #1, P. 117)

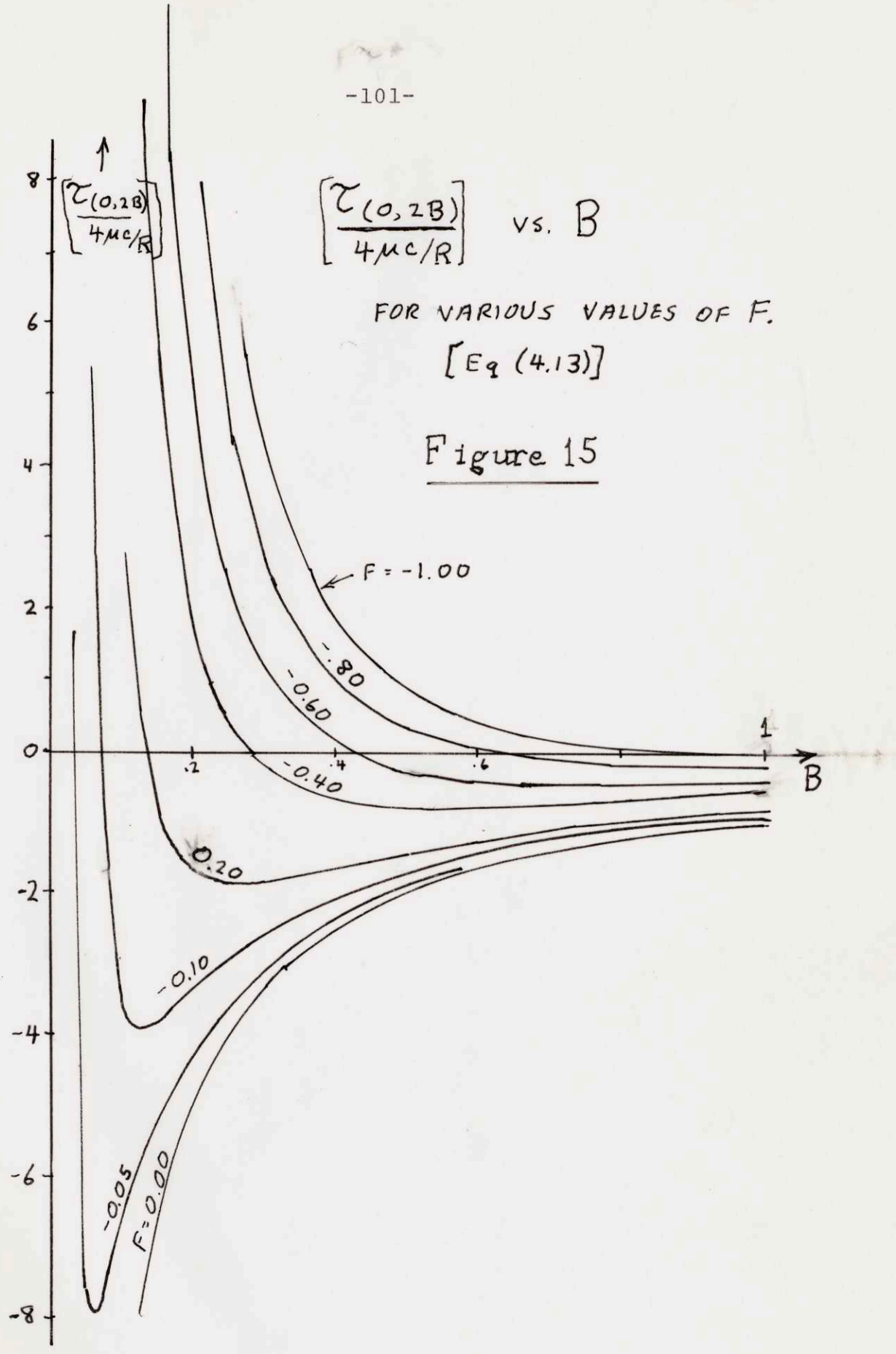
$\left[\frac{\tau_{(0,2B)}}{4\mu c/R}\right]$ vs. B
FOR VARIOUS VALUES OF F.
[Eq (4.13)]
$\left[\frac{\tau_{(0,2B)}}{4\mu c/R}\right]$
8
6
4
2
0
-2
-4
-6
-8
.2
.4
.6
1
B
F = -1.00
-.80
-0.60
-0.40
-0.20
-0.10
-0.05
F=0.00

Figure 15

Figure 16

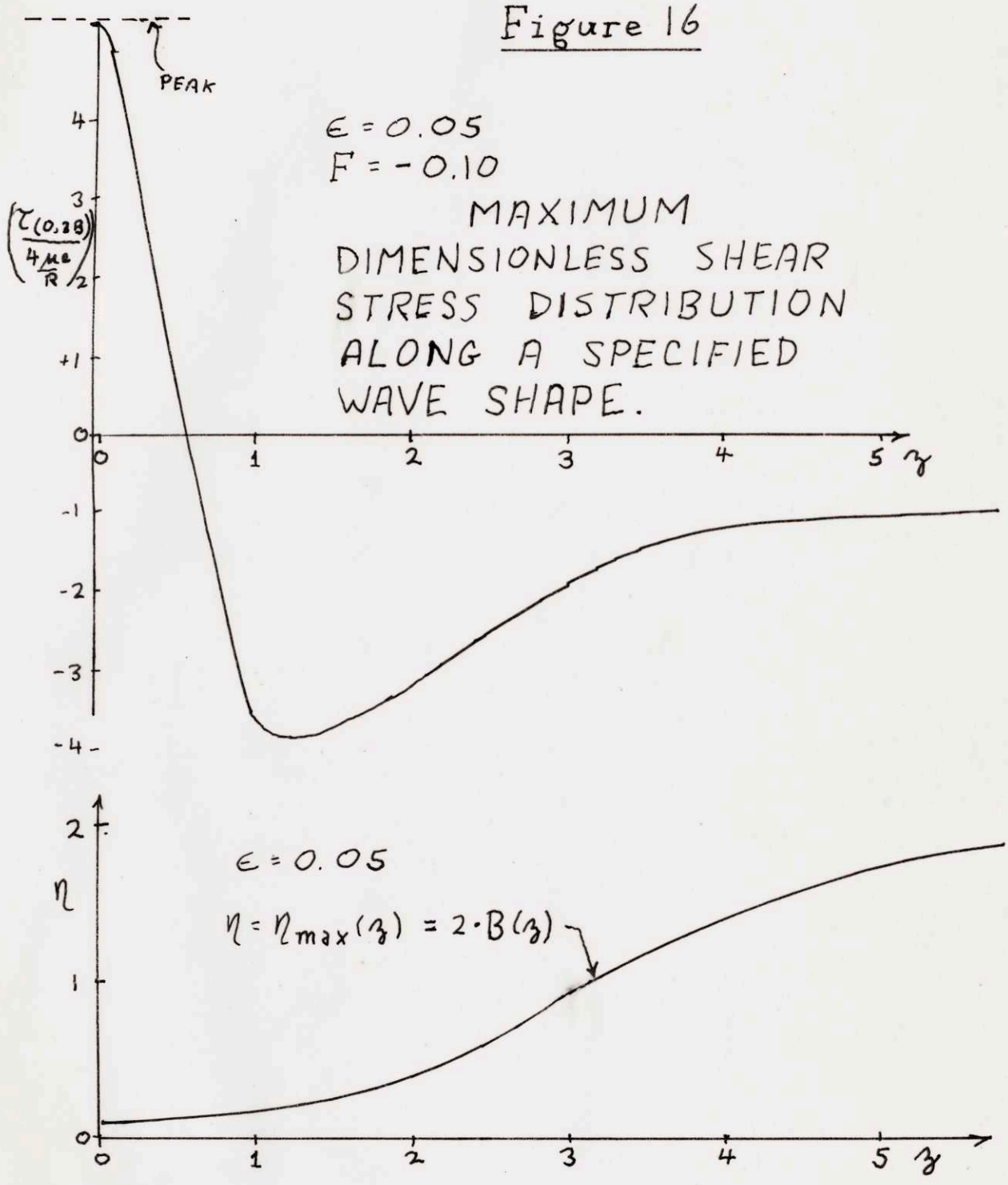
PEAK
$\epsilon = 0.05$
$F = -0.10$
MAXIMUM DIMENSIONLESS SHEAR STRESS DISTRIBUTION ALONG A SPECIFIED WAVE SHAPE.
$\left(\frac{\tau(0,z)}{\frac{4\mu a}{R}/2}\right)$
ζ
$\epsilon = 0.05$
$\eta = \eta_{max}(\zeta) = 2 \cdot B(\zeta)$
η
ζ

Figure 17

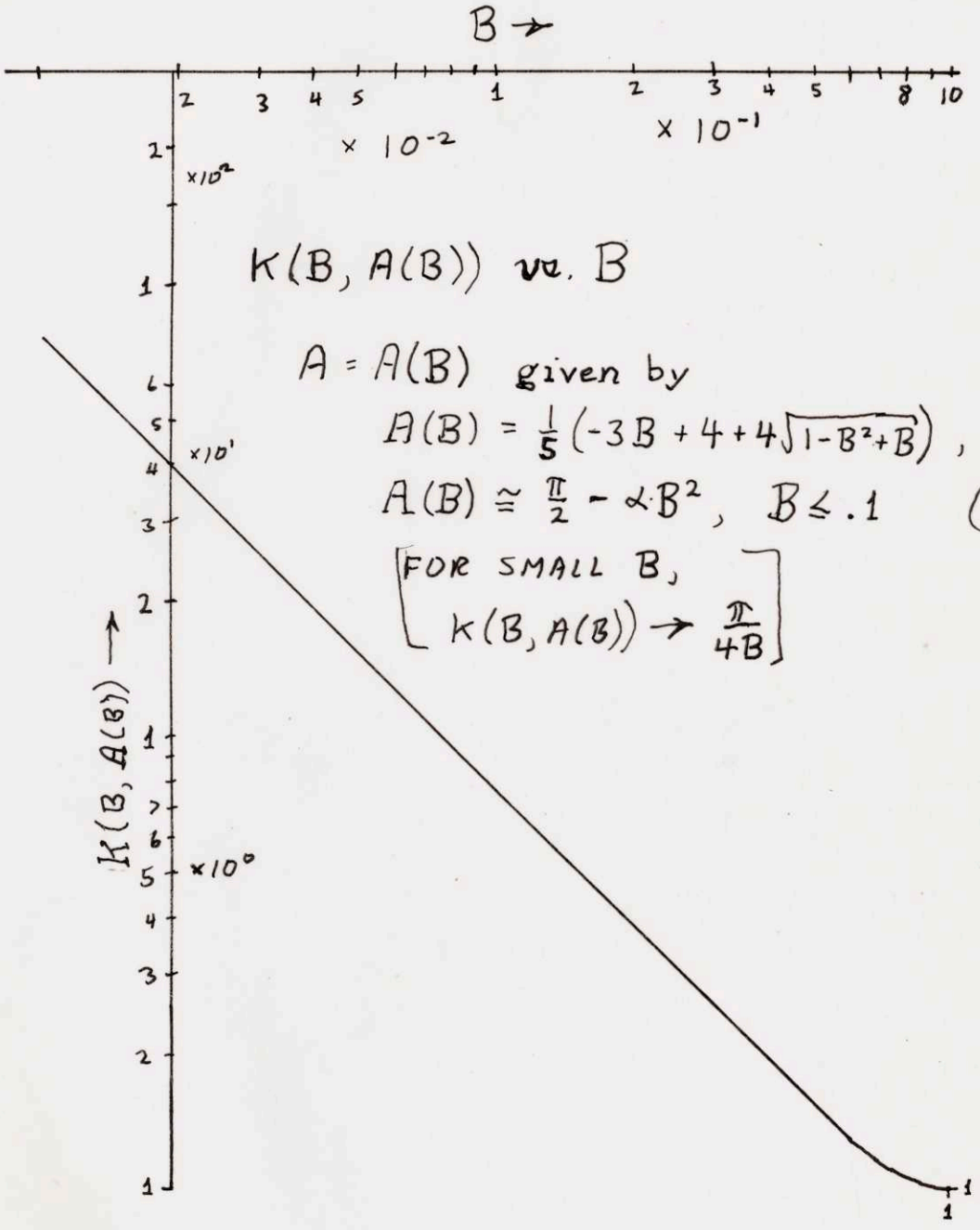
B →
2 3 4 5 1 2 3 4 5 8 10
× 10^-2
× 10^-1
K(B, A(B)) vs. B
A = A(B) given by
A(B) = 1/5 (-3B + 4 + 4√(1 - B² + B)) , B > .1
A(B) ≅ π/2 - α·B² , B ≤ .1 (α ~ 1.0)
[FOR SMALL B, K(B, A(B)) → π/4B]
K(B, A(B)) →
×10²
×10¹
×10⁰
1

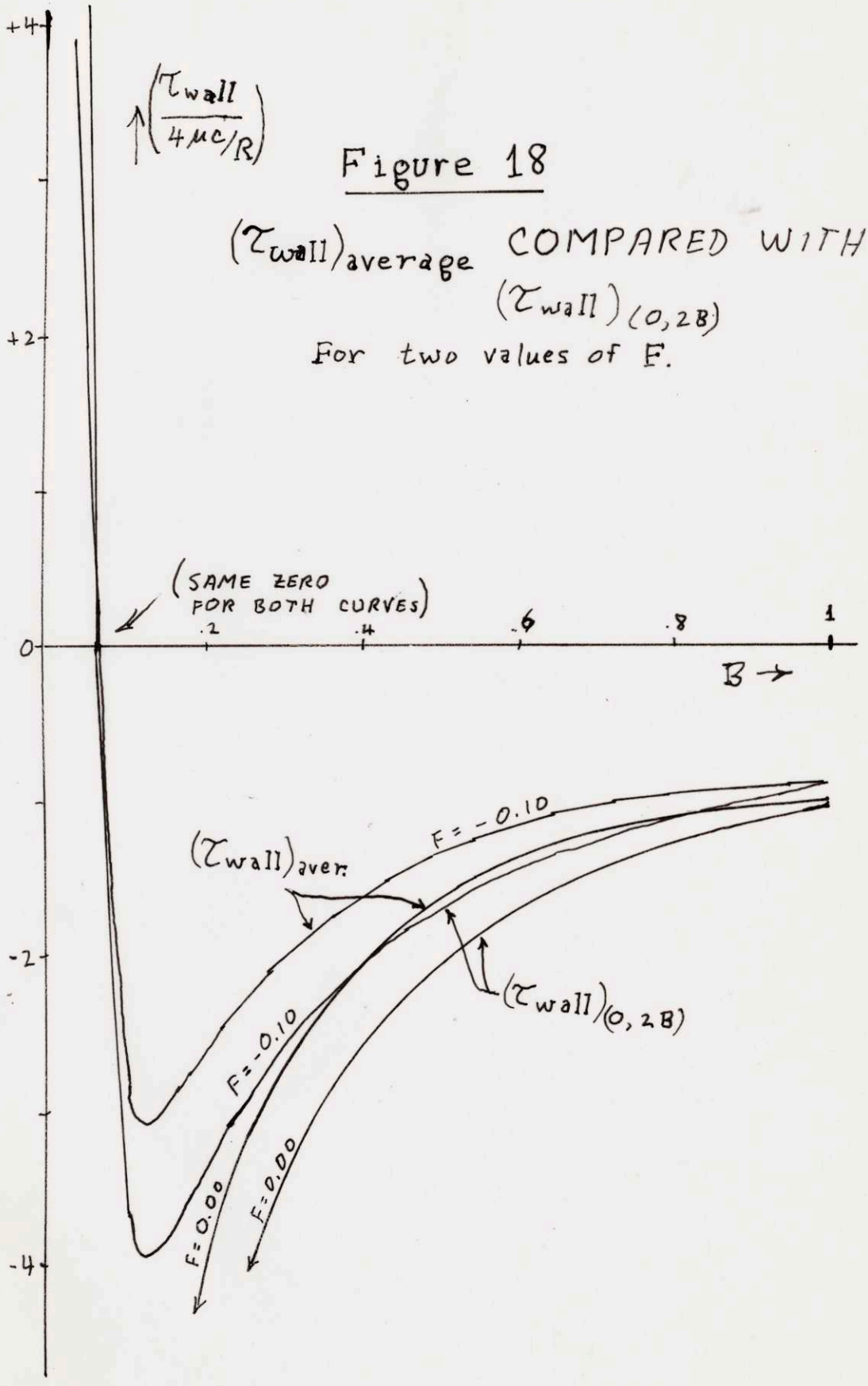

Figure 18

$(\tau_{wall})_{average}$ COMPARED WITH $(\tau_{wall})_{(0,2B)}$

For two values of F.

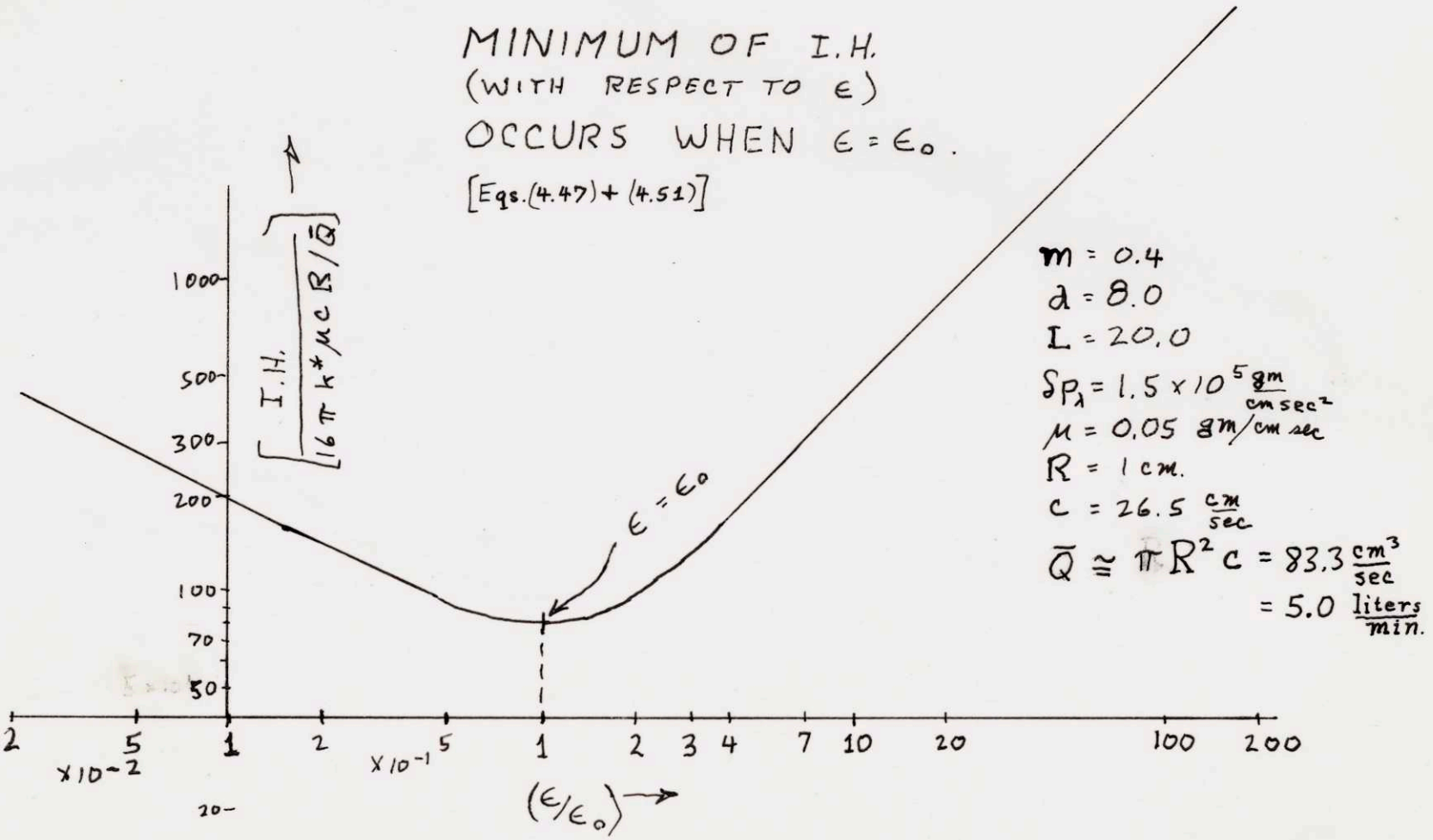
MINIMUM OF I.H.
(WITH RESPECT TO ϵ)
OCCURS WHEN ϵ = ϵ₀.
[Eqs.(4.47) + (4.51)]
m = 0.4
d = 8.0
L = 20.0
δp₁ = 1.5 x 10⁵ gm/cm sec²
μ = 0.05 gm/cm sec
R = 1 cm.
c = 26.5 cm/sec
Q̄ ≅ πR²c = 83.3 cm³/sec
= 5.0 liters/min.
I.H. / [16 π k* μc R/Q̄]
1000
500
300
200
100
70
50
20
2
5
1
2
5
1
2
3
4
7
10
20
100
200
x10⁻²
x10⁻¹
(ϵ/ϵ₀)
ϵ = ϵ₀

Figure 19

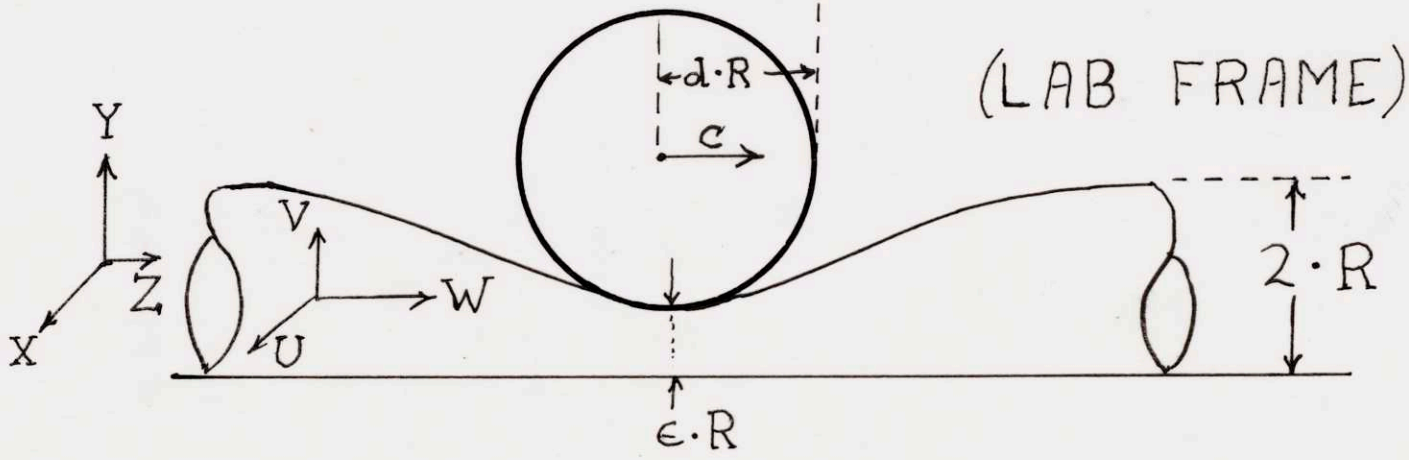

Figure 20 : For Order-of-
-Magnitude Analysis

REFERENCES

1. Blackshear, P. L., *et al.*, "Shear, Wall Interaction and Hemolysis", *Trans. Am. Soc. Art. Int. Org., 12*, 113-119, 1966.

2. *Guide to Scientific Instruments (1969-1970), Science* magazine, *165:*3900, 23 Sept. 1969.

3. "Pump-Oxygenator Equipment and Accessories" [with an accompanying undated mimeographed brochure entitled "Modular Rotating Disc Pump Oxygenator"], Med-Science Electronics, Inc., March 1, 1968.

4. "New Small-volume Peristaltic Action Pump", American Instrument Co., Inc., Bulletin No. 2340-B, November 1967.

5. "AO Heart Lung Machines", American Optical Co., Medical Division, Bulletin No. HL-001, May 1967.

6. "Sigmamotor Pumps", Sigmamotor, Inc., Catalog No. 150 (undated).

7. Sigmund A. Wesolowski, "Roller Pumps", *Mechanical Devices to assist the Failing Heart*, Chapter 8, National Academy of Sciences - National Research Council, 1966.

8. Clowes, George H. A., Jr., *et al.*, "The Physiology and Technics of Extracorporeal Circulation", June 1963. To be Chapter 13, Vol 12, of *The Practice of Surgery* .

9. Pierson, R. M., *et al.*, "Roller Pump for Artificial Hearts Using Multi-chambered Rubber Tubing", *Trans. Am. Soc. Art. Int. Org., 11*, 1965.

10. Kusserow, B. K., *et al.*, "Changes Observed in Blood Corpuscles After Prolonged Perfusions with Two Types of Blood Pumps", *Trans. Am. Soc. Art. Int. Org.*, *11*, 1965.

11. Shea, M. A., *et al.*, "The Biologic Response to Pumping Blood", *Trans. Am. Soc. Art. Int. Org.*, *13*, 1967.

12. Bernstein, E. F., Gleason, L. R., "Factors Influencing Hemolysis with Roller Pumps", *Surgery*, 432, 442, March 1967.

13. Adams, E. P., Hippisley, R. L., *Smithsonian Mathematical Formulae and Tables of Elliptic Functions* (3rd Reprint), Smithsonian Institution, Washington, D. C., 1922.

14. Schlichting, H., *Boundary-Layer Theory*, Sixth (English) Edition, [Chapter 1, Section d], Mc-Graw Hill Book Co., N.Y., 1968.

15. Shapiro, A. H., Jaffrin, M. Y., Weinberg, S. L., "Peristaltic Pumping with Long Wave Lengths at Low Reynolds Number", *Journal of Fluid Mechanics*, *37*, 799-825, 1969.

16. Shapiro, A. H., "Pumping and Retrograde Diffusion in Peristaltic Waves", *Proceedings of a Workshop on Ureteral Reflux in Children*, National Acad. of Sci-National Res. Council, Wash., D. C., 109-133, 1967.

17. Flink, E. B., and Watson, C. J., "A Method for the Quantitative Determination of Hemoglobin and Related Heme Pigments in Feces, Urine, and Blood Plasma",

Jour. of Biological Chemistry, 146, 171, 1942.

18. Bluestein, M., and Mockros, L. F., "Hemolytic Effects of Energy Dissipation in Flowing Blood", *Medical and Biological Engineering, 7,* 1-16, 1969.

19. Guyton, A. C., *Textbook of Medical Physiology,* Third Edition, W. B. Saunders Co., Philadelphia, 1966.

20. Abramowitz, M., and Stegun, I. A., *Handbook of Mathematical Functions with Formulas, Graphs and Mathematical Tables,* National Bur. of Standards, Washington, D. C., 1964.

21. Dwight, H. H., *Tables of Integrals and Other Mathematical Data* (Fourth Edition), Macmillan Co., N.Y., 1961